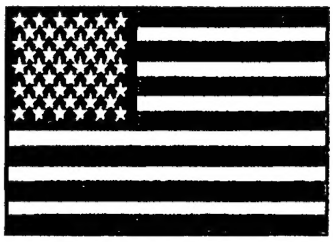

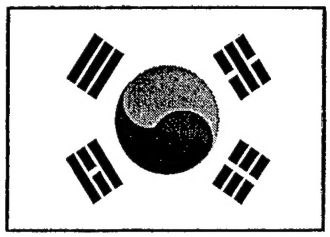

Contract Report SL-97-1
UAST-CR-93-005

JOINT U.S./ROK R&D PROGRAM FOR NEW UNDERGROUND AMMUNITION STORAGE TECHNOLOGIES

FINAL REPORT

EXPLOSION EFFECTS MODELING OF SELF-SEALING UNDERGROUND EXPLOSIVE STORAGE CHAMBER DESIGNS

by

Ali Amini, Eugene L. Foster
Colin J. Shellum

UTD Incorporated
8560 Cinderbed Road, Suite 1300
Newington, VA 22122

February 1997

Prepared for U.S. Army Engineer Waterways Experiment Station
3909 Halls Ferry Road
Vicksburg, Mississippi 39180-6199

PRINTED ON RECYCLED PAPER

Joint U.S./ROK R&D Program for New Underground Ammunition Storage Technologies

Contract Report SL-97-1
February 1997

Explosion Effects Modeling of Self-Sealing Underground Explosive Storage Chamber Designs

by Ali Amini, Eugene L. Foster, Colin J. Shellum

UTD Incorporated
8560 Cinderbed Road, Suite 1300
Newington, VA 22122

Final report

Approved for public release; distribution is unlimited

Prepared for U.S. Army Engineer Waterways Experiment Station
3909 Halls Ferry Road
Vicksburg, MS 39180-6199

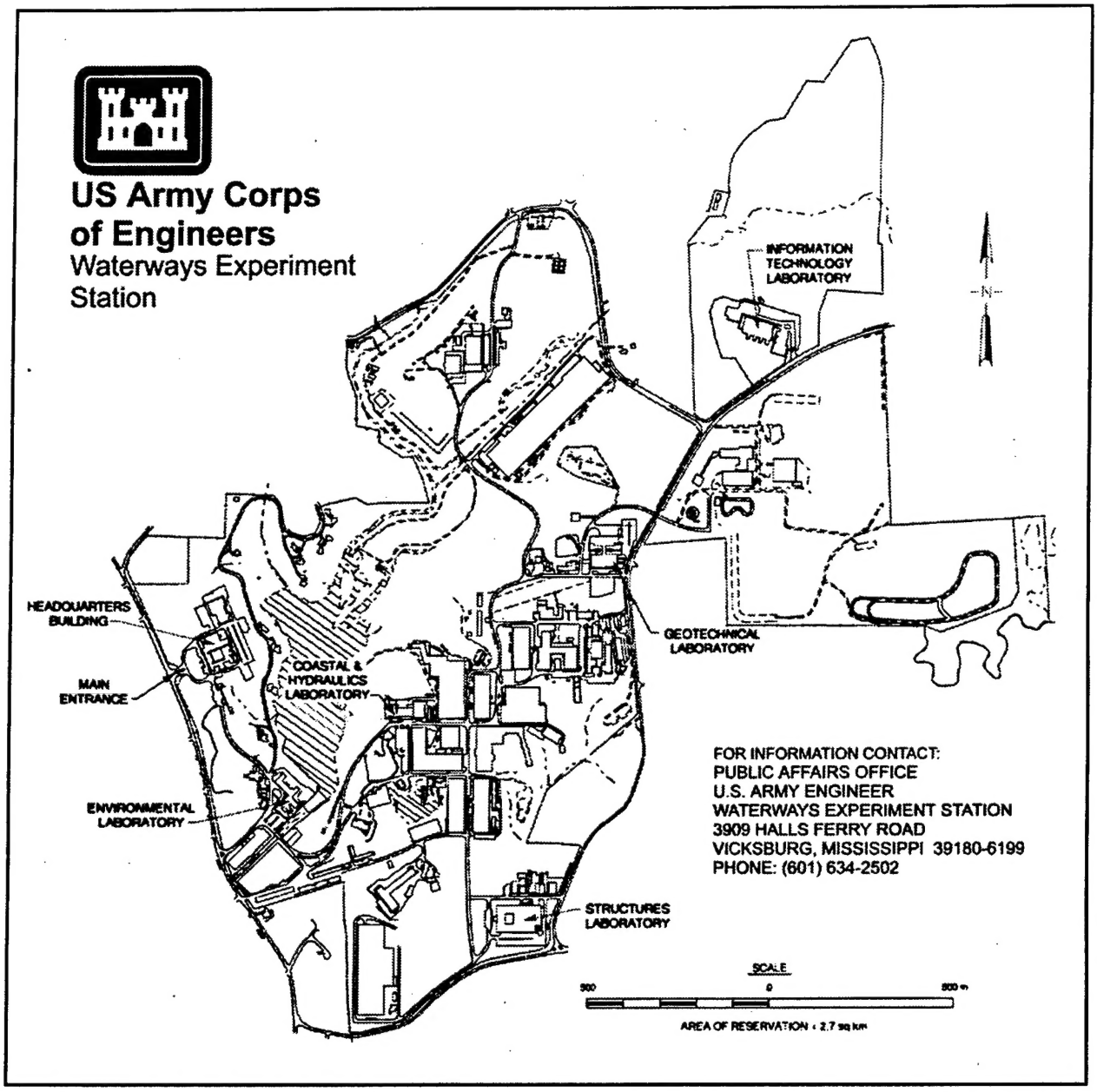

Waterways Experiment Station Cataloging-in-Publication Data

Amini, Ali.

Explosion effects modeling of self-sealing underground explosive storage chamber designs / by Ali Amini, Eugene L. Foster, Colin J. Shellum ; prepared for the U.S. Army Engineer Waterways Experiment Station.

60 p. : ill. ; 28 cm. — (Contract report ; SL-97-1)

Includes bibliographical references.

"UAST-CR-93-005"—Cover.

1. Explosives — Storage — Mathematical models. 2. Blast effect — Safety measures —Mathematical models. 3. Ammunition containers — Safety measures — Mathematical models. 4. Explosions — Safety measures — Mathematical models. I. Foster, Eugene L. II. Shellum, Colin J. III. United States. Army. Corps of Engineers. IV. U.S. Army Engineer Waterways Experiment Station. V. Structures Laboratory (U.S. Army Engineer Waterways Experiment Station) VI. Joint U.S. /ROK R&D Program for New Underground Ammunition Storage Technologies. VII. Title. VIII. Series: Contract report (U.S. Army Engineer Waterways Experiment Station) ; SL-97-1.

TA7 W34c no.SL-97-1

PREFACE

The U.S./ROK R&D Program for New Underground Ammunition Storage Technologies was sponsored by the U.S. Army Technical Center for Explosives Safety. This study was conducted for the U.S. Army Engineer Waterways Experiment Station (WES) under contract DACA39-93-C-0010 as part of the Joint U.S./Korea R&D Study for New Underground Ammunition Storage Technologies. Technical Managers for the joint program were Mr. Landon K. Davis, Geomechanics and Explosion Effects Division (GEED), WES, Structures Laboratory (SL), and Dr. So-young Song, Korean Agency for Defense Development. The Program Managers were Mr. Gary W. Abrisz, U.S. Army Technical Center for Explosives Safety, and COL Yeon Woo Chung, Logisitics Bureau, Korean Ministry of Defense.

Dr. Ali Amini, UTD, Inc., conducted the study reported herein, assisted by Dr. Eugene L. Foster, and Mr. Colin J. Shellum, coauthors of this report. The work was monitored by Mr. Charles E. Joachim, GEED. Dr. Jimmy P. Balsara was Chief, GEED, and Mr. Bryant Mather was Director, SL.

At the time of preparation of this report, Director of WES was Dr. Robert W. Whalin. Commander was COL Bruce K. Howard, EN.

TABLE OF CONTENTS

LIST OF FIGURES

LIST OF FIGURES (CONTINUED)

LIST OF TABLES

CONVERSION FACTORS, NON-SI TO SI (METRIC)
UNITS OF MEASUREMENT

Non-SI units of measurement used in this report can be converted to SI (metric) units as follows:

Multiply	By	To Obtain
degrees	0.01745329	radians
degrees Fahrenheit	{5/9}{F - 32}	Celsius (C)
degrees Celsius	C + 273.15	Kelvin (K)
feet	0.3048	metres
feet per second	0.3048	metres per second
feet per second-squared	0.3048	metres per second-squared
inches	25.4	millimetres
pounds (mass)	0.4535924	kilograms
pounds (mass) per cubic foot	16.01846	kilograms per cubic metre
pounds (force) per square inch	0.006894757	megapascals

1.0 INTRODUCTION

1.1 General

Most countries store military ammunition supplies in above-ground, earth-covered magazines. Military safety regulations in the U.S. and the Republic of Korea require that large areas of land around ammunition storage sites be designated as exclusion areas to protect personnel and structures from the hazards of an accidental magazine explosion. In many areas of Korea and the U.S., high population densities and intensive land use make such hazard areas expensive to acquire, and encumber large tracts of land that could be more profitably used for other purposes.

The Joint U.S.Korea R&D Program for New Underground Ammunition Storage Technologies is a five-year cooperative research effort designed to greatly reduce the needed hazard areas for ammunition storage by developing new design concepts for underground magazines which can contain, within the underground area, most of the hazardous effects of an accidental explosion. The underground magazine would consist of storage chambers and access tunnels excavated in rock geologies.

One proposed method for containing the effects of an explosion is the "self-sealing" chamber concept. In this concept, one wall of the storage chamber would be designed to fail under the pressure of a detonation in the chamber, and would be pushed into a portion of the chamber access tunnel which passes near the chamber wall, thus blocking the escape of the airblast shock and detonation gas flow. The purpose of the study reported here was to investigate the technical feasibility of the self-sealing chamber concept.

In this analysis, it was desired to predict the physical events associated with an accidental explosion in an underground storage chamber in order to determine the optimal storage chamber design. Design criteria for this concept require that the explosive storage chamber be self-sealing during an accidental explosion, with no adverse impacts on the stability of adjacent storage areas, (including sympathetic detonation), and no significant amount of airblast or debris reaching the surface from the tunnel entrance portal.

The objective of this project was to address these needs by developing an explosion effects simulation model for various self-sealing chamber configurations. The basic premise of the self-seal concept involves a large "plug" which either slides or fails into the access drift opening driven by the force of the detonation of the stored explosives. The primary issues to be addressed by the model included:

- ability of the self-seal plug to move into the opening;
- speed at which the plug moves;
- plug integrity after the blast, and;
- influence of various chamber configurations on explosion effects.

Another objective of this study was to make recommendations regarding pre-construction and post-event field measurements, and subsequent calibration of the predictive models. As a consequence of these investigations, an alternative means of self-sealing was considered to improve performance and re-access. This alternative consists of a sliding blast door.

The modeling effort permitted the evaluation of the self-sealing chamber concept feasibility, and will ultimately provide a means of performance prediction through calibration of model behavior by scaled tests and measurements or rock mass characterization during full scale construction. The Universal Distinct Element Code (UDEC) developed by Itasca Consulting Group {[1] was used for modeling the behavior of the self-sealing plug during the dynamic event. The pressure function due to an explosion and rate of mass flow of hot gases out of the storage chambers were calculated using a thermodynamic model developed by UTD personnel.

1.2 Scaled Test Scenarios and Modeling

The Waterways Experiment Station plans to conduct a 1/3-scale test for sealing of accidental explosions at the Linchburg mine in Magdalena Mountains, Socorro County, New Mexico. A plan view of the site is shown in Figure 1. According to this figure a sliding block will be constructed at the entrance to Chamber 1. The block will be cut from the surrounding rock and the floor of the chamber so that the only resistance to its movement in addition to its inertia will be friction along its contact with the floor of the chamber.

Chamber 3 will be connected to the north test drift by a curved chamber access drift. In addition, the wall between the chamber and the straight portion of the access drift will be weakened over a portion of its length. This will be achieved by cutting at least four slots along the entire width of the wall so that a block of rock resting freely on the floor of the chamber is created. In this scenario the resisting forces include the inertia of the wall and the friction along the contact surface of the block with the floor of the chamber. Chambers 6 and 7 along the South Test Drift may have weakened walls similar to Chamber 3.

1.3 Organization of the Report

In Section 2, the results of the geologic investigation of the test site carried out by UTD are presented. The models used for predicting the behavior of the self-sealing plugs are reviewed in Section 3 with a discussion of the means of collecting the input data. In Section 4, the results of the model runs are presented together with a discussion of results. The concept for an alternative sealing system is presented in Section 5, and Section 6 presents recommendations for pre-blast and post-blast field measurements, and calibration of the prediction models.

2.0 TEST SITE GEOLOGY

2.1 General Geology

The Linchburg Mine is in the Magdalena Mining District and is located about 5 miles south

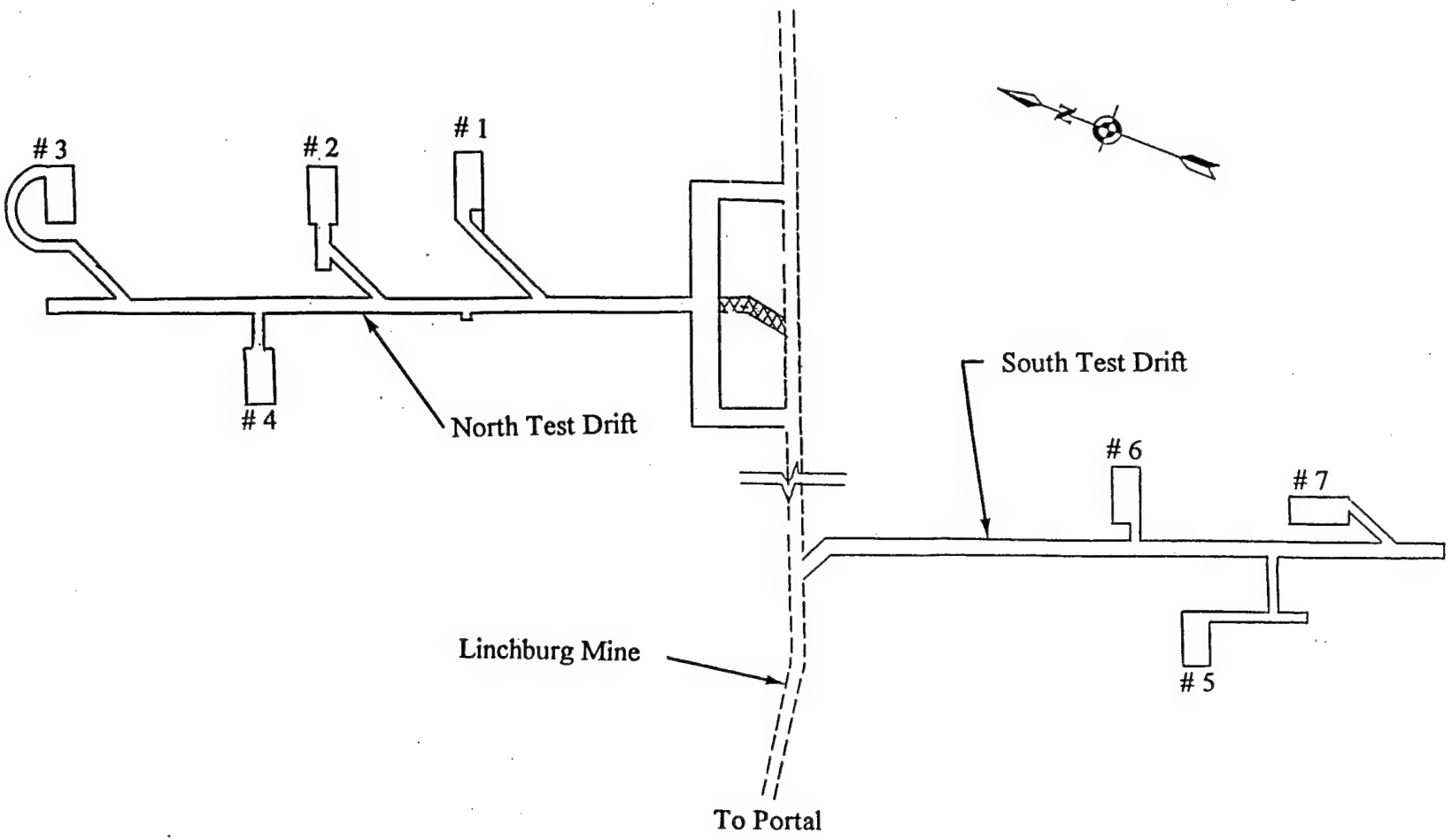

Figure 1. Layout of test chambers for U.S. 1/3-scale explosion containment tests.

of Magdalena, New Mexico. Figure 2 (modified from Corps of Engineers "Preliminary" dated 3/17/93) is a generalized geologic map and shows the plan outline of the proposed excavation.

As shown in Figure 2 there are two sets of test chambers, one on each side of the existing mine drift. The spatial separation of the two sets conveniently leads to individual analyses and classification of the two local rock masses, which have been labeled Region A, and Region B. The detailed geologic report for the site is presented in Appendix A. Figures 4-9 of the Appendix show the geology of each region. The jointing patterns shown in these figures are directly input into the numerical model used for modeling of the storage chambers during the dynamic event.

2.2 Rock Mass Quality

The rock mass quality of the site was quantified by the Rock Mass Rating (RMR) method, and the Norwegian Geotechnical Institutes's Q system. The RMR number ranged from 57 to 61, indicating fair to good quality rock [2]. The Q number was calculated as 7.8, indicating a good quality rock as well [3]. Individual parameters and calculation procedures for both the RMR and Q systems are shown in Tables 1 and 2, respectively. Based on the RMR and Q numbers, the stand-up times for the drifts and chambers are estimated to be more than two years. This indicates that major support systems may not be necessary during the construction phase of the site except at sharp intersection points between access drifts.

The RMR and Q systems provide means for quantifying some of the in-situ properties of the rock mass. As an example, the joint roughness and alteration numbers of the Q system are used to calculate the angle of friction along the surface of a joint set as shown in Section 3.2. In addition, the SRF number for the Q system shown in Table 2 may be modified for high stress conditions during the dynamic event. In this case, a Q number is achieved for stability of chamber walls under the explosive loading. This Q number may further be used to specify a support system for the walls.

The RMR and Q systems can be supplemented with field-measured convergence data taken during excavation to calibrate the models used for simulation of the dynamic event. The calibrated model can then be used for analysis of the actual site after the rock mass quality of the site is determined, and convergence measurements are made during its excavation phase.

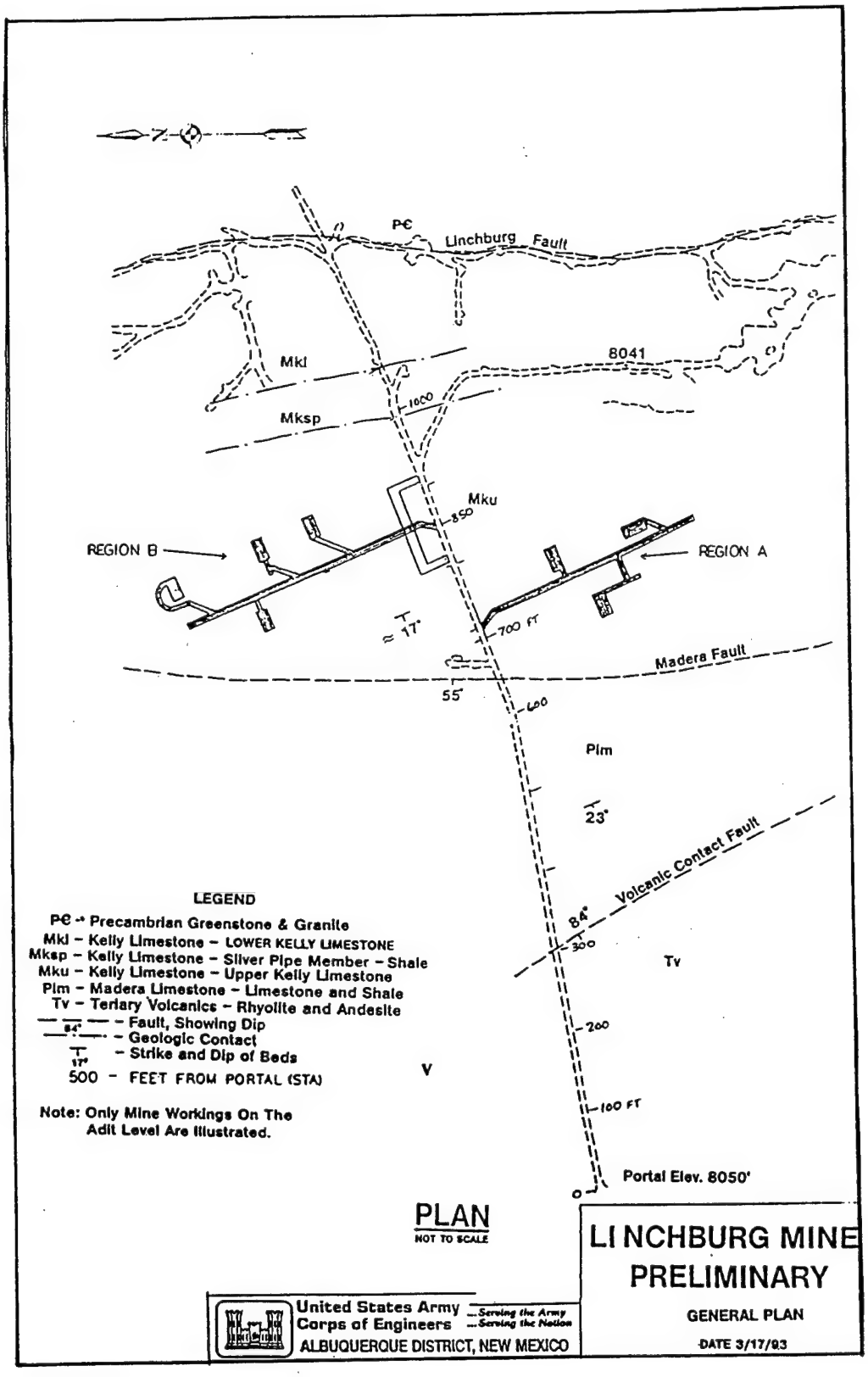

Figure 2. General geologic map of Linchburg Mine.

Table 1. Rock Mass Rating (RMR) system calculations.

GEOMECHANICS CLASSIFICATION SYSTEM (ROCK MASS RATING SYSTEM)				
PARAMETER	VALUE	REGION A	REGION B	COMMENTS
1. INTACT ROCK STRENGTH	100 MPa	10	10	estimated value
2. RQD	75-90%	17	17	
3. DISCONTINUITY SPACING	200-600mm	10	10	
4 DISCONTINUITY CONDITION	Rough, slightly weathered. High persistence, separation <1mm	20	22	Region A slightly more weathered than B
5. GROUNDWATER	Dry to damp	10	12	Region A slightly more damp than B
TOTAL RMR		67	71	
6. DISCONTINUITY ORIENTATION	Varies by location	-10	-10	Range from fair to unfavorable to very unfavorable; unfavorable = -10
ADJUSTED RMR		57	61	
CLASSIFICATION		III FAIR ROCK	II GOOD ROCK	Region A on the high side of fair. Region B on the low side of good.

Table 2. Q system calculation of the Q number.

Q SYSTEM RATING		
PARAMETER	**RATING**	**COMMENTS**
1. RQD	80	
2. J_n, Joint Set Number	9	3 Joint Sets
3. J_r, Joint Roughness Number	1.75	smooth to rough
4. J_a, Joint Alteration	2.0	faily tight, calcite mineralized
5. J_w, Joint Water	1.0	dry or minor flow
6. SRF, Stress Reduction Factor	1.0	medium stress, $\frac{\sigma_c}{\sigma_1} \approx \frac{100}{6} \approx 18$
$Q = \frac{RQD}{J_n} \cdot \frac{J_r}{J_a} \cdot \frac{J_w}{SRF} = \frac{80}{9} \cdot \frac{1.75}{2} \cdot 1 = 7.8$		

3.0 OVERVIEW OF PREDICTION MODELS

3.1 Modeling Approach

The self-seal scenarios can be modeled both analytically and numerically. The analytic approach is based on the application of Newton's second law to a block of rock, i.e:

$$F = m\ a \tag{1}$$

where F = the net force acting on the block,
m = mass of the block, and
a = acceleration of the block.

If the block is cut off from the wall of the chamber on all sides as shown in Figure 3, then the net force, F, acting during the dynamic event is:

$$F = \Delta P \cdot A - \mu \cdot W \tag{2}$$

where ΔP = the average differential dynamic pressure acting on the block face with area A,
μ = coefficient of friction between the rock block, and the floor of the chamber, and
W = weight of the rock block.

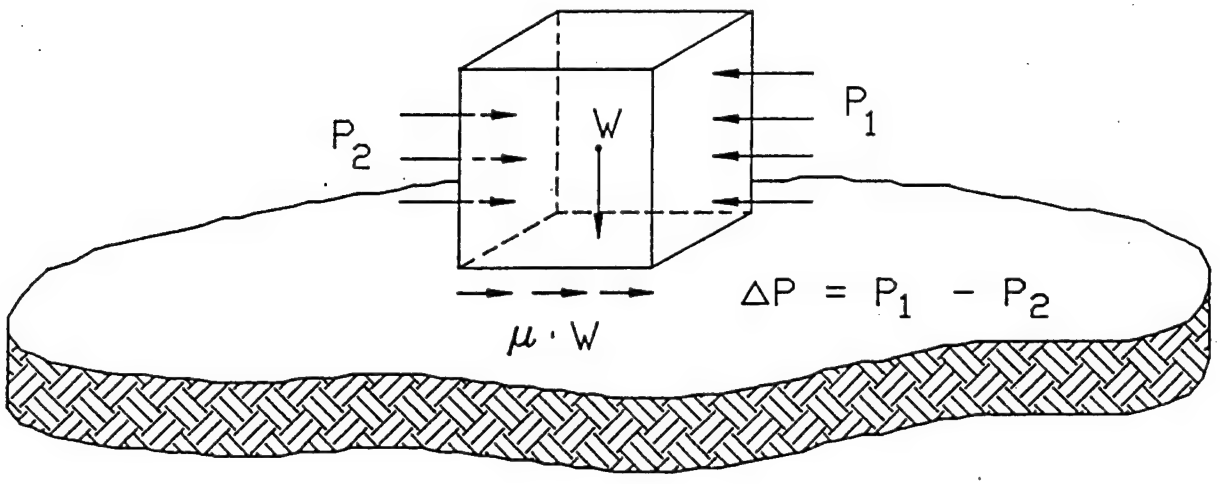

cah04

Figure 3. Forces acting on a rock block

The displacement of the rock block under the dynamic differential pressure, ΔP, can then be calculated by integrating the acceleration term obtained from Eq.(2) twice with respect to time.

The analytic method described above is appropriate when the weak wall acts as a solid mass under the dynamic load. However, if the weak wall is jointed, the wall may not behave as a solid mass, but as a discontinuum, with blocks of rock breaking off and ejecting into the access drifts. For this purpose it is necessary to use a numerical code suitable for discontinuum modeling. UDEC is a two-dimensional discontinuum code which simulates the response of discontinuous media by assuming that the media consist of blocks of rock in contact with each other through normal and tangential springs. The displacement of the blocks is calculated by solving the equations of motion of the blocks explicitly in a time-marching fashion.

The tangential force, F_t, between blocks is limited by the Mohr-Coulomb friction law:

$$F_t \quad C \quad F_n \tan \phi \tag{3}$$

where C = cohesion of the joint,
F_n = normal force on the joint, and
ϕ = angle of friction of the joint.

The normal force is usually set to zero in tension for non-welded joints. In compression the normal force is limited by the tolerance on overlap between blocks in contact.

3.2 Input Data for Modeling with UDEC

A model of the weak wall in UDEC is generated by cutting a cross-section of the wall into small rock blocks created by the existing joints and those purposely created during construction. Then the intact rock and joint properties are specified. The accidental explosion is then modeled by applying a time-varying differential pressure function on the chamber side of the weak wall. Figure 4 shows a typical UDEC model. When the rock mass is blocky, movements along existing joints will dominate the displacement of the wall. As a result, the input parameters of importance are the number of joint sets, orientation of joint sets, spacing of individual joints, and resistance along the joints. The material properties of the intact rock needed by UDEC are its density, bulk modulus, and shear modulus. Typical property values for the intact rock in a blocky rock mass may be selected from those published in the literature.

Field observations of the joint parameters are reduced to mean values with variance over a certain range. A qualitative description of joint roughness and alteration, also collected during a site visit, is evaluated to determine joint roughness which may vary from joint set to joint set. Further interpretation leads to determination of joint resistance (or the joint friction angle where rough surfaces indicate higher friction angles). These data used in the Q system provide a means for quantifying the joint friction for constructibility and design purposes by assigning a rating number based on degree of joint roughness (J_r), and joint alteration (J_a), and using the following equation [4]:

$$J_f = \tan^{-1}\left(\frac{J_r}{J_a}\right) \tag{4}$$

where J_f = angle of joint friction.

In addition to joint properties, the blast pressure acting on the wall as a function of time is needed for input to UDEC. This pressure is generated due to explosion of the munitions in the confinement of the storage chamber. The following section presents a method for calculating this pressure function.

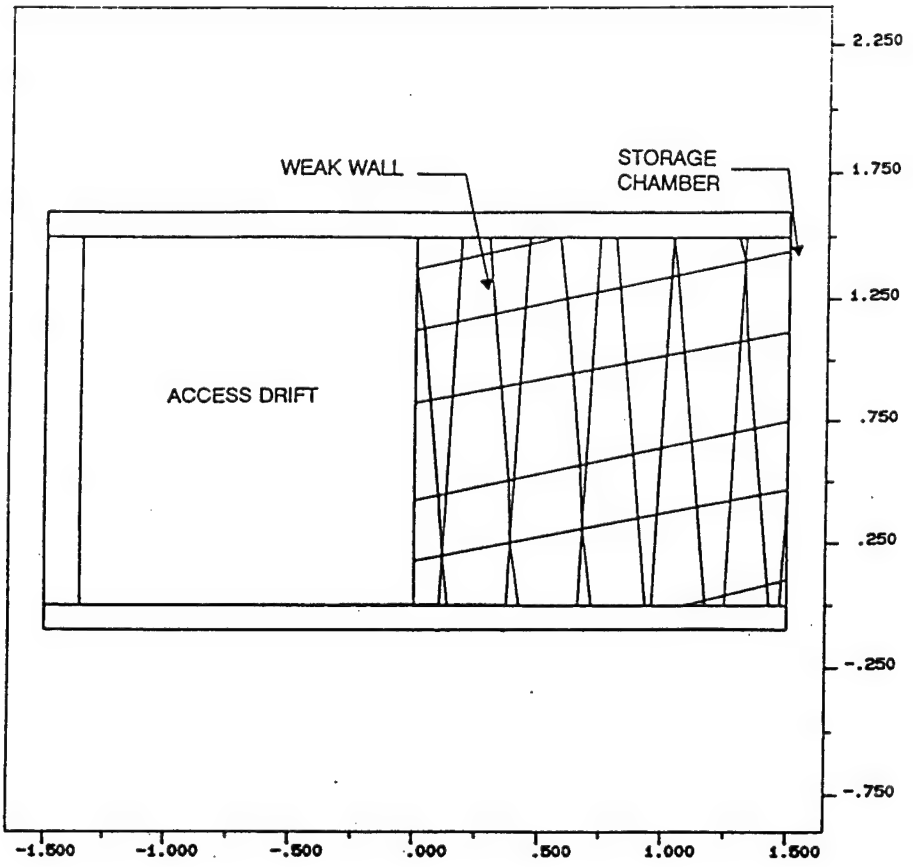

Figure 4. A typical UDEC model

3.3 Thermodynamic Model

The gas pressure inside the chamber reaches a peak value at the moment of detonation. Over time, the explosion-generated gases start flowing out of the chamber opening (blowdown), thereby reducing the pressure inside the chamber. When a sliding block exists at the opening to

the chamber (throat area), the block moves under the differential gas pressure, and chokes off the throat within a short time increment. The effectiveness of the self-seal concept depends on the volume of hot gases escaping the chamber before it is completely choked by the sliding block.

The variable pressure inside the chamber can be calculated through a thermodynamic analysis of the blowdown process and the variable throat area. The first variable needed for the thermodynamic analysis is the peak pressure inside the chamber which can be calculated, knowing the weight and type of the explosive and the chamber volume, using the CONWEP program [5]. Then an incremental analysis in time domain can proceed by calculating the gas temperature from the perfect gas law:

$$T_1 \quad \frac{P_1 V_c}{M_1 R} \tag{5}$$

where T = gas temperature,
P = gas pressure,
V_c = chamber volume,
M = gas mass, and
R = specific gas constant.

Note that the subscript 1 in Eq.(5) refers to variables at the beginning of the time increment. Knowing the gas temperature, the velocity of gases (V_t) through the throat area (A_t) can be determined by the following equation:

$$V_t \quad \sqrt{2g\ (778\ )\ C_p(T_1 \quad T_t)} \tag{6}$$

where g = acceleration due to gravity,
C_p = specific heat at constant pressure, and
$T_1 - T_t$ = temperature change from chamber to throat.

The temperature change may be calculated as:

$$T_1 \quad T_t \quad T_1\left(1 \quad \left(\frac{P_t}{P_1}\right)^{\frac{k\,1}{k}}\right) \tag{7}$$

Where k = C_p/C_v, and
C_v = specific heat at constant volume.

The change in the mass of gases, ΔM, inside the chamber is then calculated as:

$$\Delta M \quad \frac{C\, A_t\, V_t\, \Delta t}{v_t} \tag{8}$$

where C = contraction coefficient for the throat,
A_1 = variable throat area,
V_t = gas velocity,
Δt = duration of the time increment, and
v_t = specific volume of gases at the throat.

The temperature of gases inside the chamber drops due to the work done by the gas as it is forced out of the throat and the work done on the sliding block as it moves under the gas pressure. The change in temperature, ΔT, can be quantified as follows:

$$\Delta T \quad \frac{W_G}{M_2}\frac{W_B}{C_V} \tag{9}$$

where W_G = work done by gas through the throat,
W_B = work done by the gas on the sliding block, and
M_2 = mass of gas at the end of the time increment = $M_1 - \Delta M$

With the change in temperature, and mass of the gas inside the chamber known over the time increment of interest, the gas pressure at the end of the time increment, P_2 can be calculated as:

$$P_2 \quad \frac{M_2\, R\, T_2}{V_c} \tag{10}$$

where T_2 = gas temperature at the end of time increment = $T_1 - T_1$.

The pressure, temperature, and mass of the gas at the end of the current time increment are then used as the initial values over the next time increment, and the incremental analysis in time domain continues. This leads to the pressure function acting on the chamber walls and the rate of mass flow of the gas from the chamber.

Note that in the above incremental analysis, the throat area, A_1, varies in a sliding block scenario. The change in A_1 is calculated from the block displacement predicted by UDEC. On the other hand, the gas pressure calculated through the thermodynamic model is an input to UDEC. This indicates that the thermodynamic analysis and UDEC modeling for a sliding block at the throat (Chamber 1) have to be carried out in a coupled approach. For other chambers A_1 remains constant and the pressure function can be determined before running UDEC models. Figures 5 and 6 show the results of the thermodynamic analysis for Chamber 6.

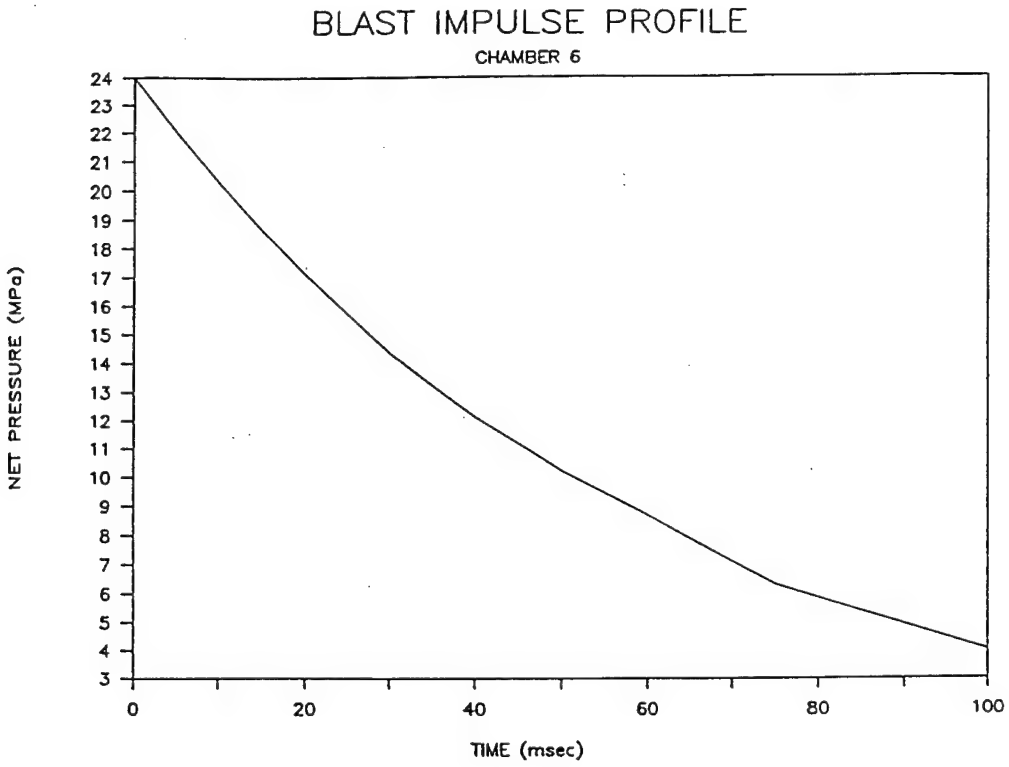

Figure 5. Blast impulse profile.

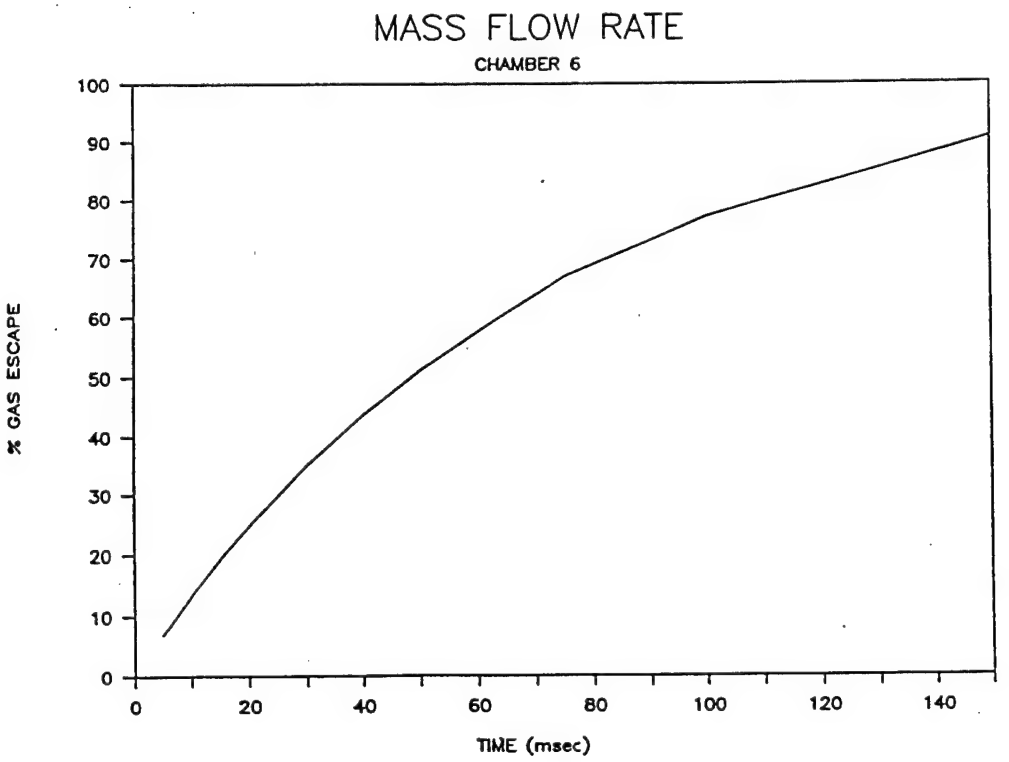

Figure 6. Rate of mass flow from chamber.

4.0 SELF-SEAL SCENARIO MODELING

4.1 Assumptions and Modeling Results

Chambers 1, 3, 6, and 7 were modeled using UDEC. The rock mass surrounding these chambers was assumed to be similar to that observed along the main portal drift during the site visit by UTD. Detailed geology of the rock mass around each chamber can be determined accurately after each chamber is excavated. At the time of writing of this report, this detailed information is not available.

For Chamber 1 it was assumed that a sliding block exists at the entrance to the chamber as shown in Figure 1. The block is cut from adjacent walls, the crown, and the floor of the chamber, and rests on a horizontal sliding plane on top of the chamber floor. The only contact force on the block was assumed to be due to friction between the block and the chamber floor. Figures 8-10 show the UDEC model of a section of the wall, the displaced wall due to the dynamic load, and wall displacement and mass flow of hot gases out of the chamber as a function of time.

Chamber 3 was assumed to have a weak wall section as shown in Figure 11. This weak wall is generated by cutting four slots on the two sides, the top and the bottom of the wall, so that the only contact force acting on the wall is due to friction at the base of the wall. To study the effects of weak wall thickness, thicknesses of 1.5m and 2.5m were modeled. Figures 12-14 show the UDEC model of the wall and the displacement and mass flow curves for the 1.5m and the 2.5m wall thickness.

Chamber 7 was assumed to have a weak wall similar to Chamber 3. Figures 15 and 16 show the plan view of the chamber and its displacement and mass flow curves respectively. For this chamber the weak wall would seal the gases in the main access drift. However, in Figure 16, only the mass flow rate out of the chamber is presented. Chamber 6 was analyzed without any weak walls or sliding blocks. This was done to determine the stability of the chamber walls under the dynamic loading event. Note that in chambers where the wall is weakened over a fraction of its length, the rest of the wall which is intact has to be checked for stability under blast loading. Figures 17 and 18 show the plan view of Chamber 6, and the spalling of its wall during the dynamic loading event. Using the Q system described in Section 2, with an SRF of 20 for rockburst conditions, a Q value of 0.4 is obtained. This is an indication of a very poor rock mass under the dynamic event as illustrated by the UDEC model of Figure 18. Based on the Q system, tensioned rock bolts are necessary for stability of chamber walls.

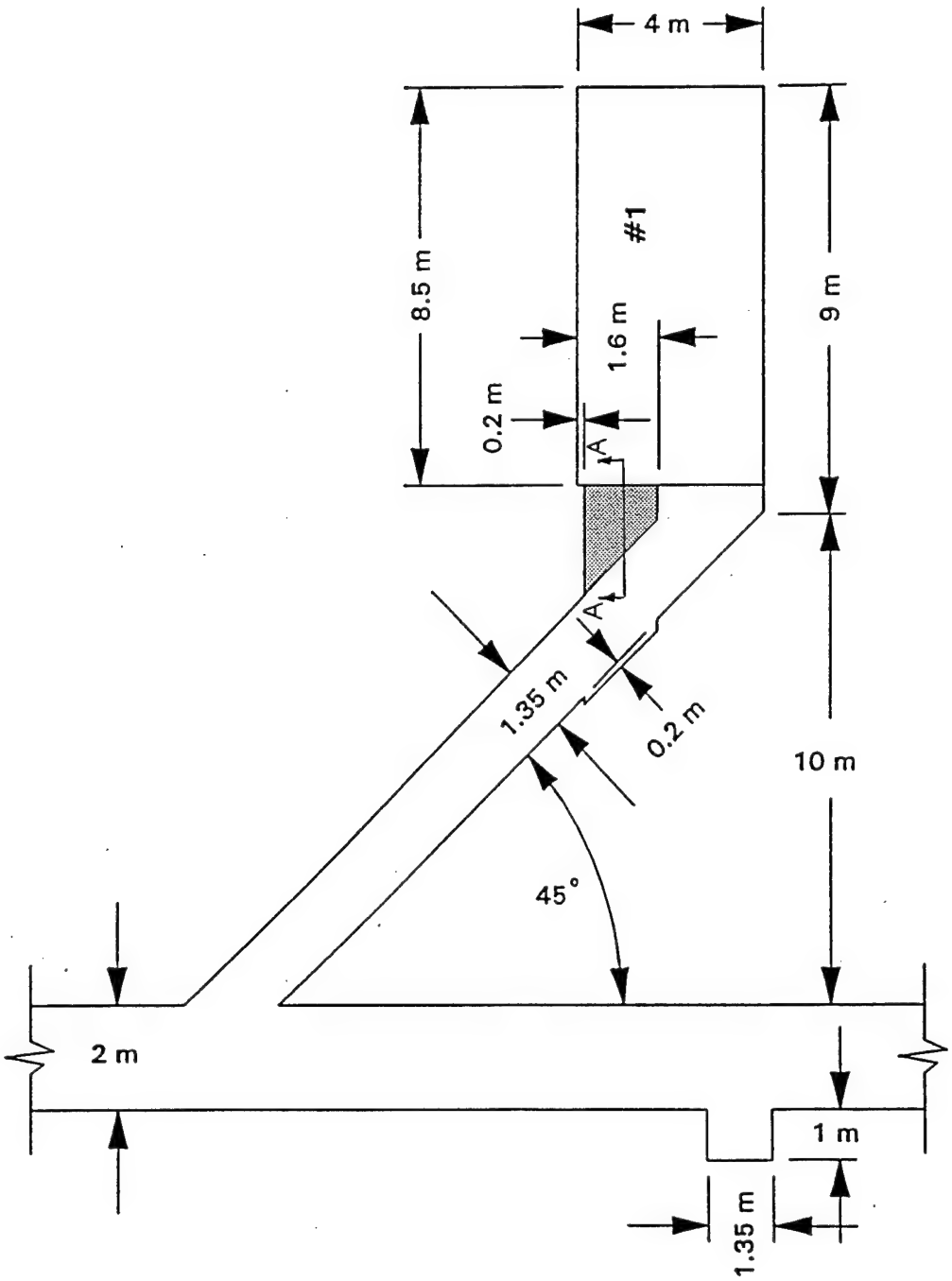

Figure 7. Plan view of Chamber 1.

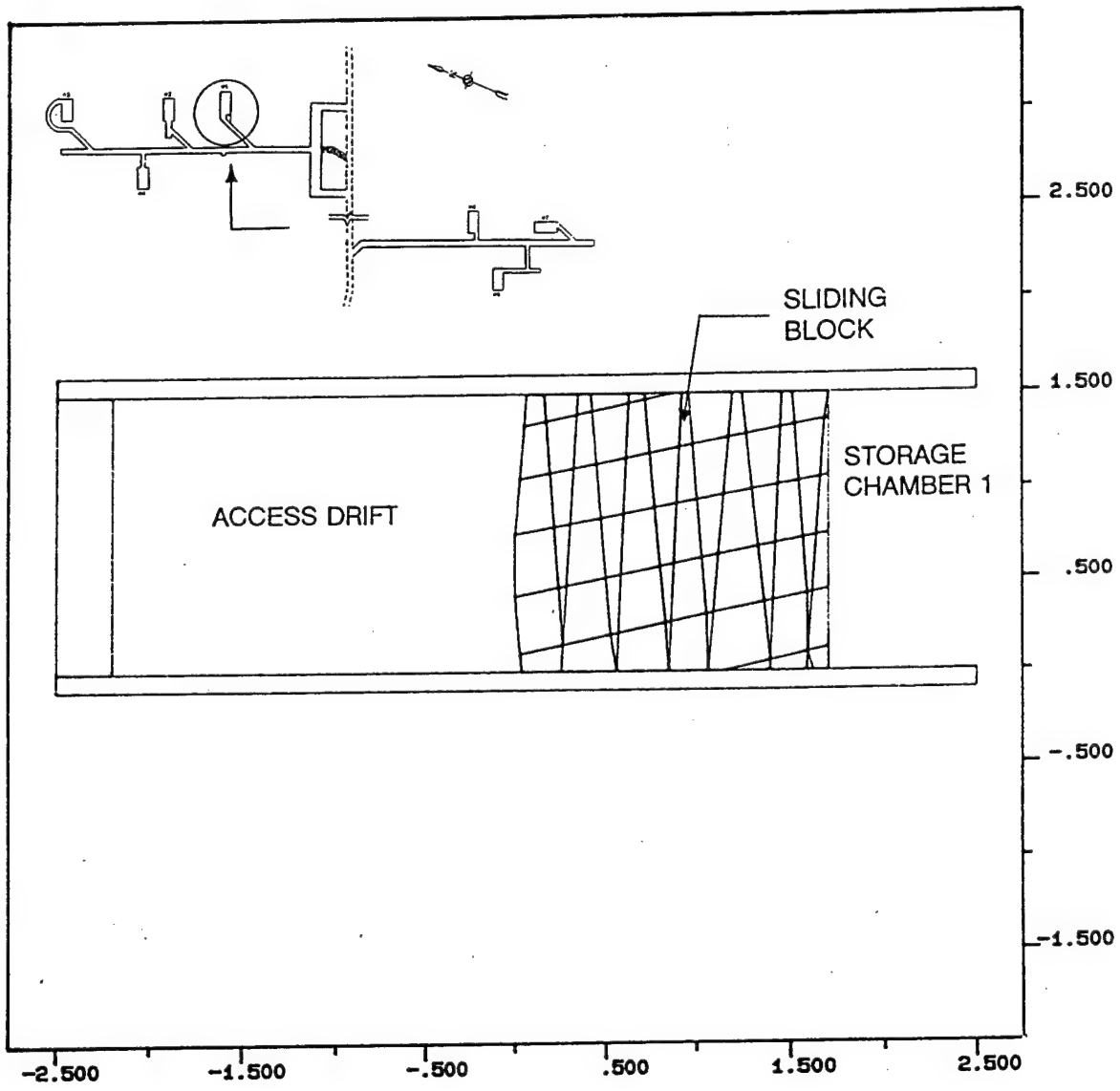

Figure 8. UDEC model of the sliding block in Chamber 1 (along section A-A of Figure 7).

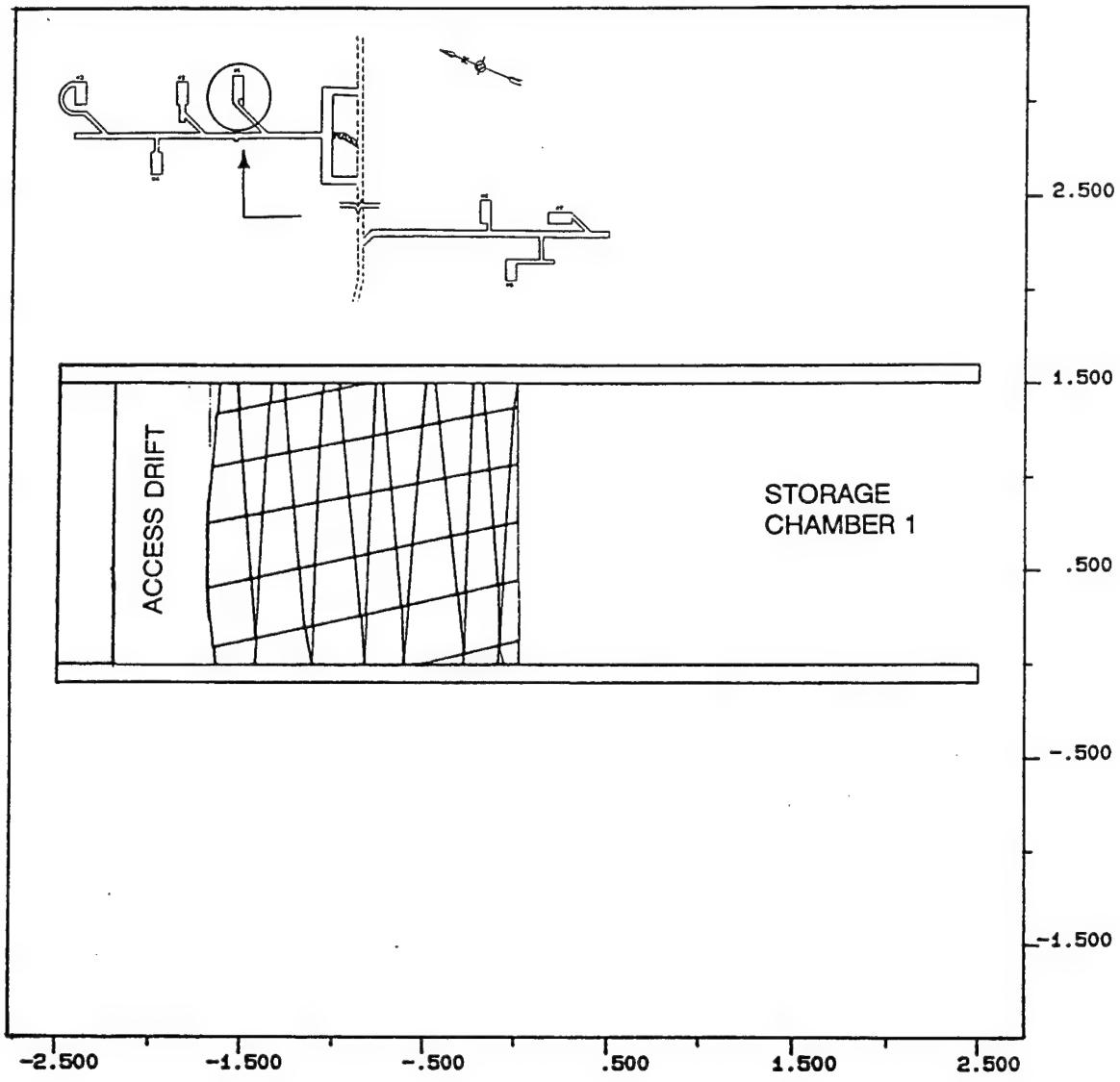

Figure 9. Displacement of sliding block in Chamber 1.

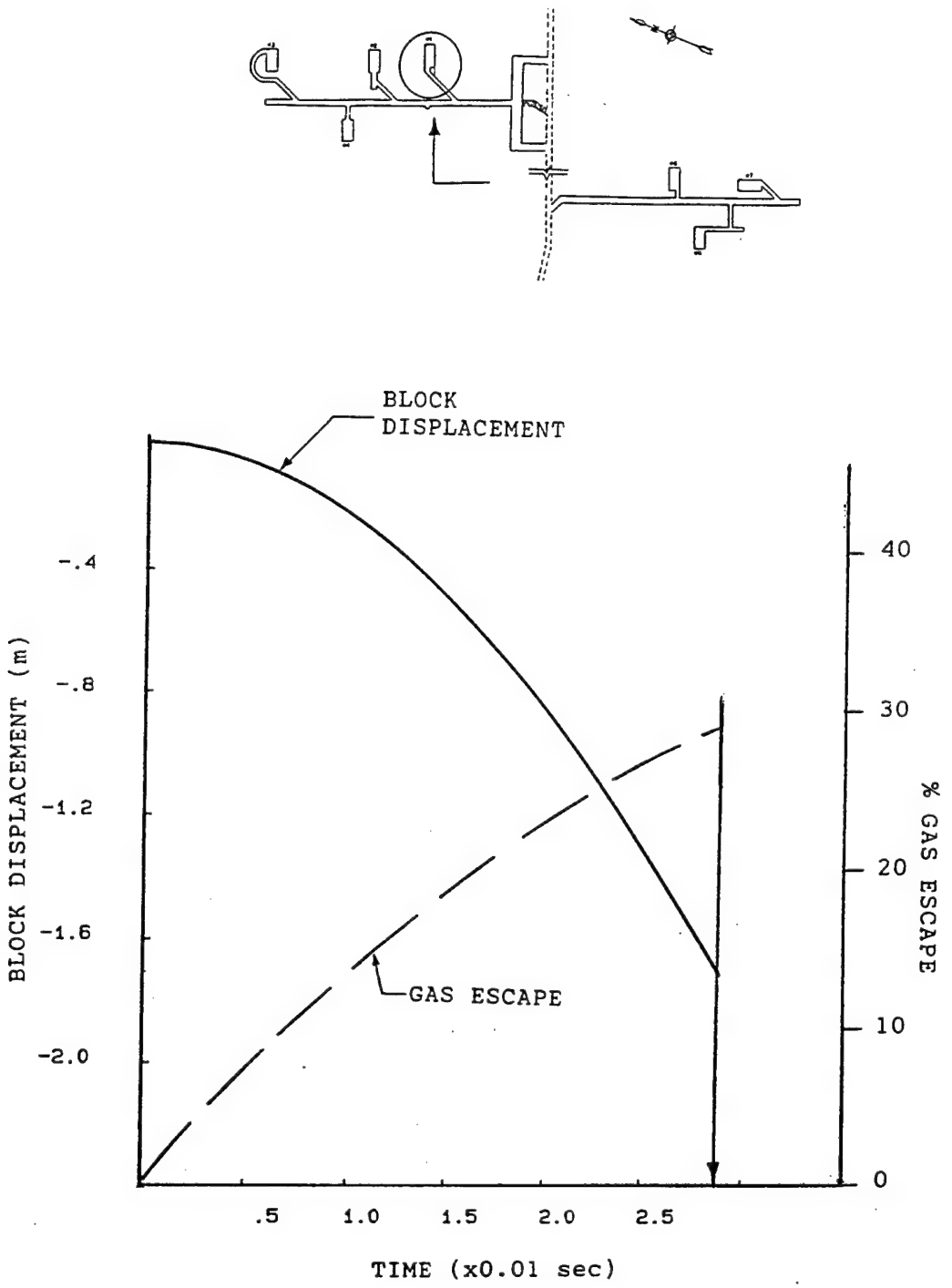

Figure 10. Displacement and mass flow rates for Chamber 1.

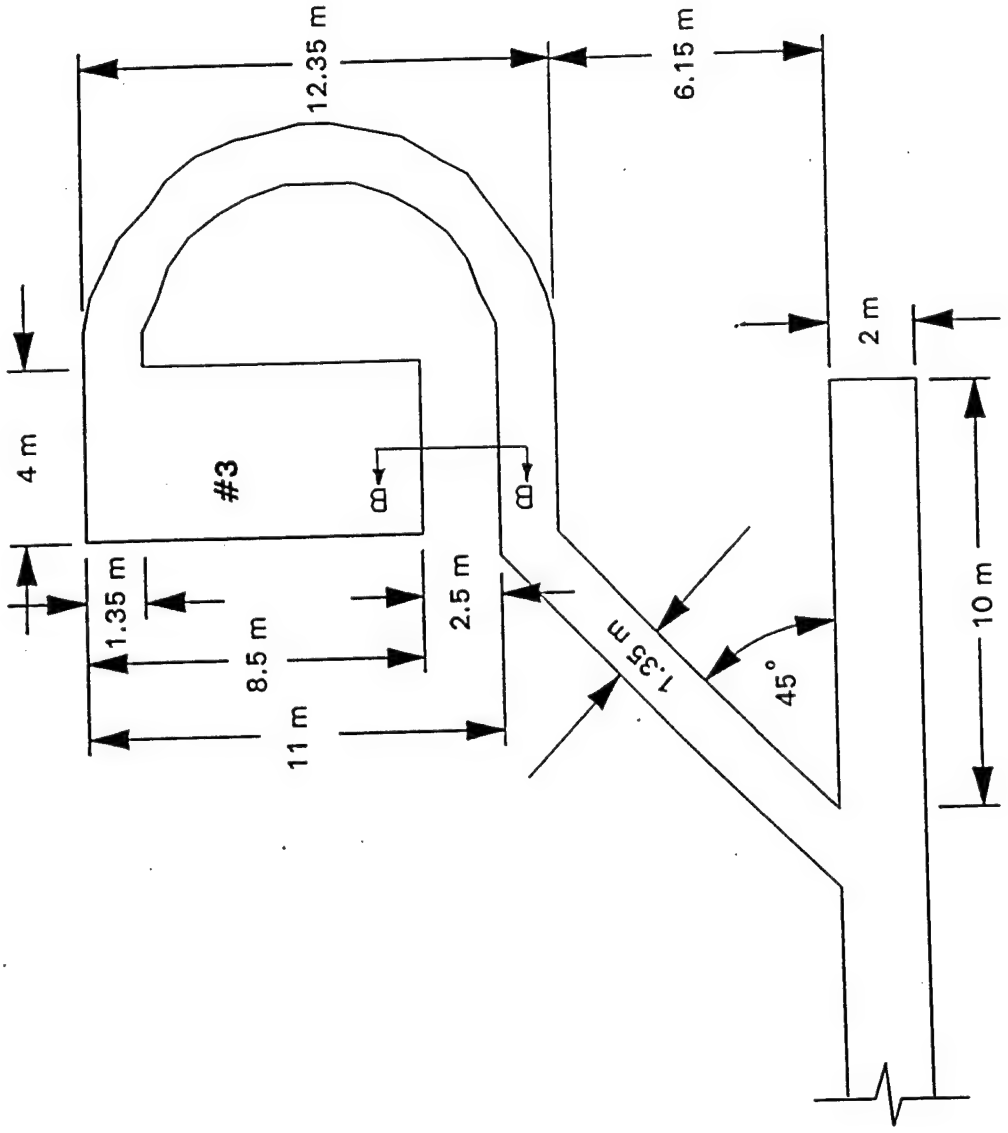

Figure 11. Plan view of Chamber 3.

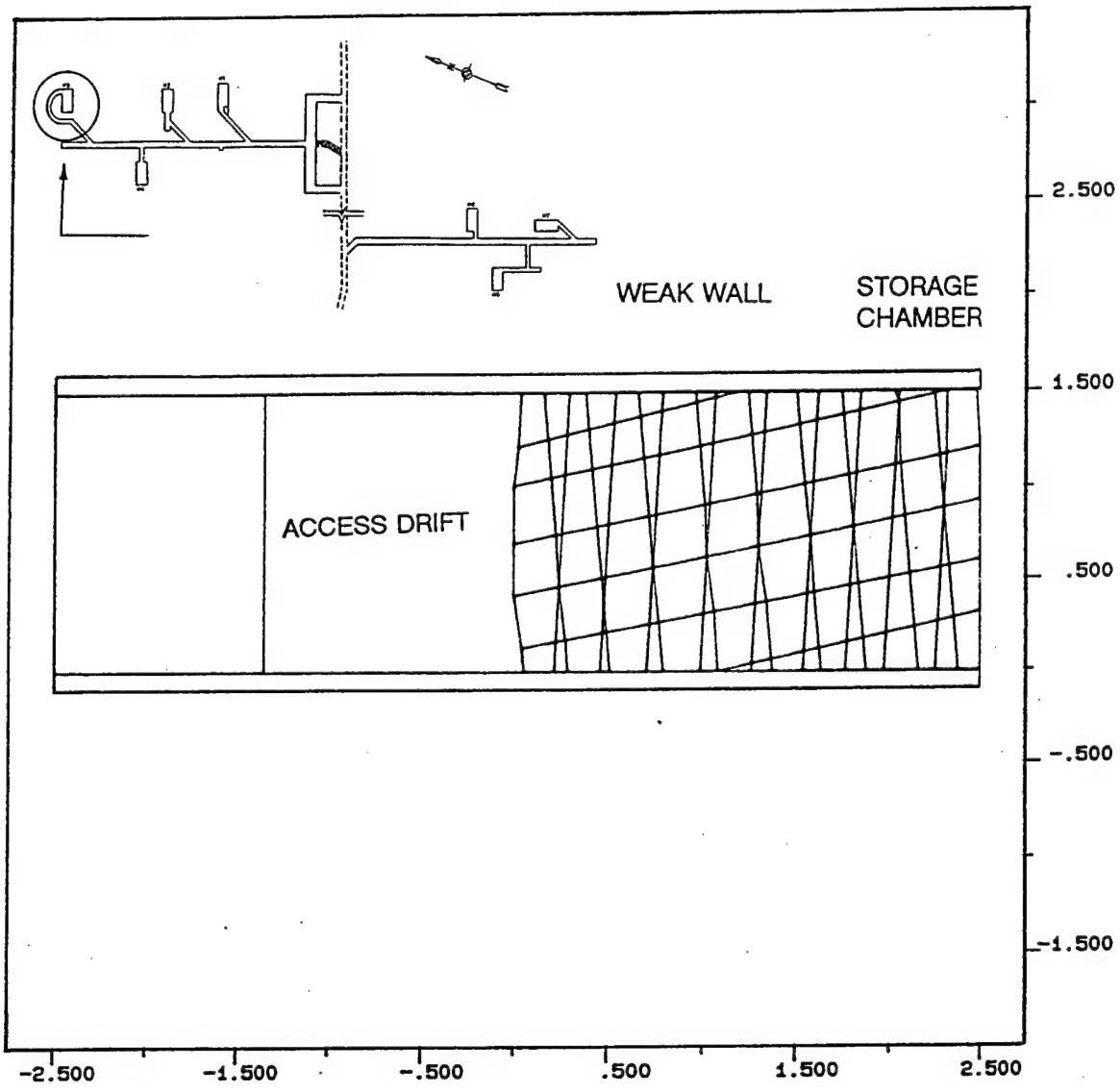

Figure 12. UDEC model of the weak wall in Chamber 3 (along section B-B of Figure 11).

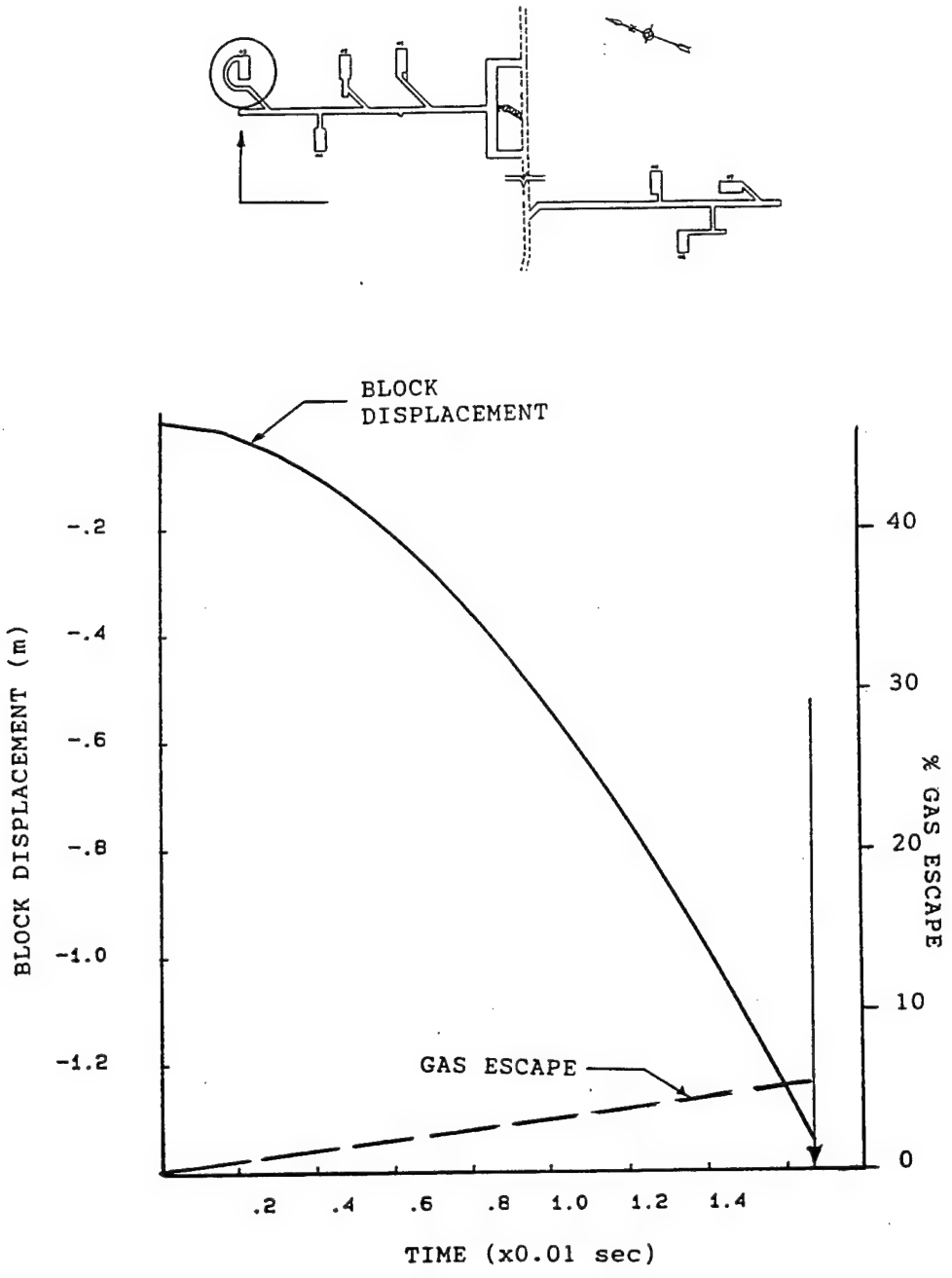

Figure 13. Wall displacement and mass flow out of Chamber 3 (1.5m width).

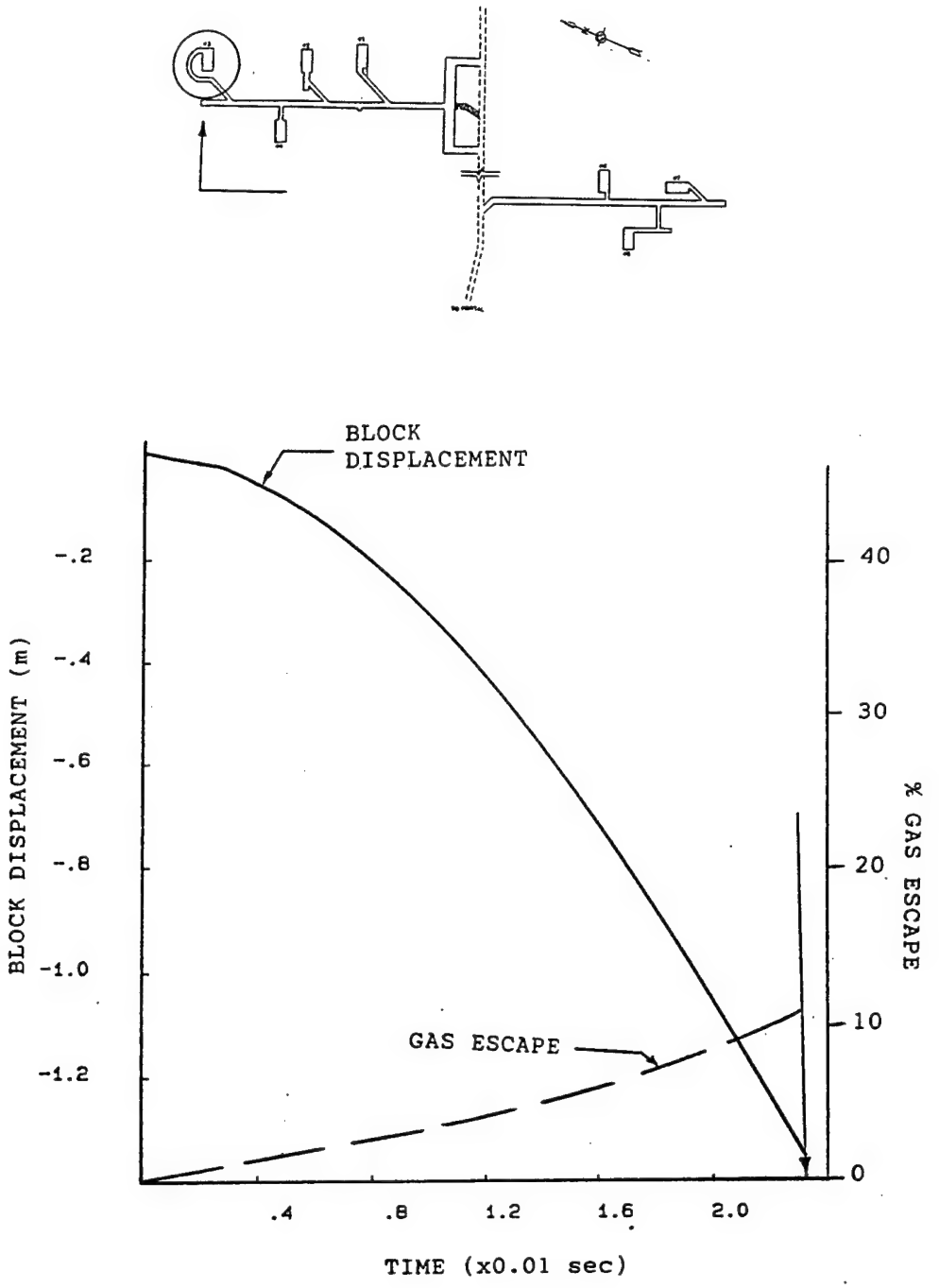

Figure 14. Wall displacement and mass flow out of Chamber 3 (2.5m width).

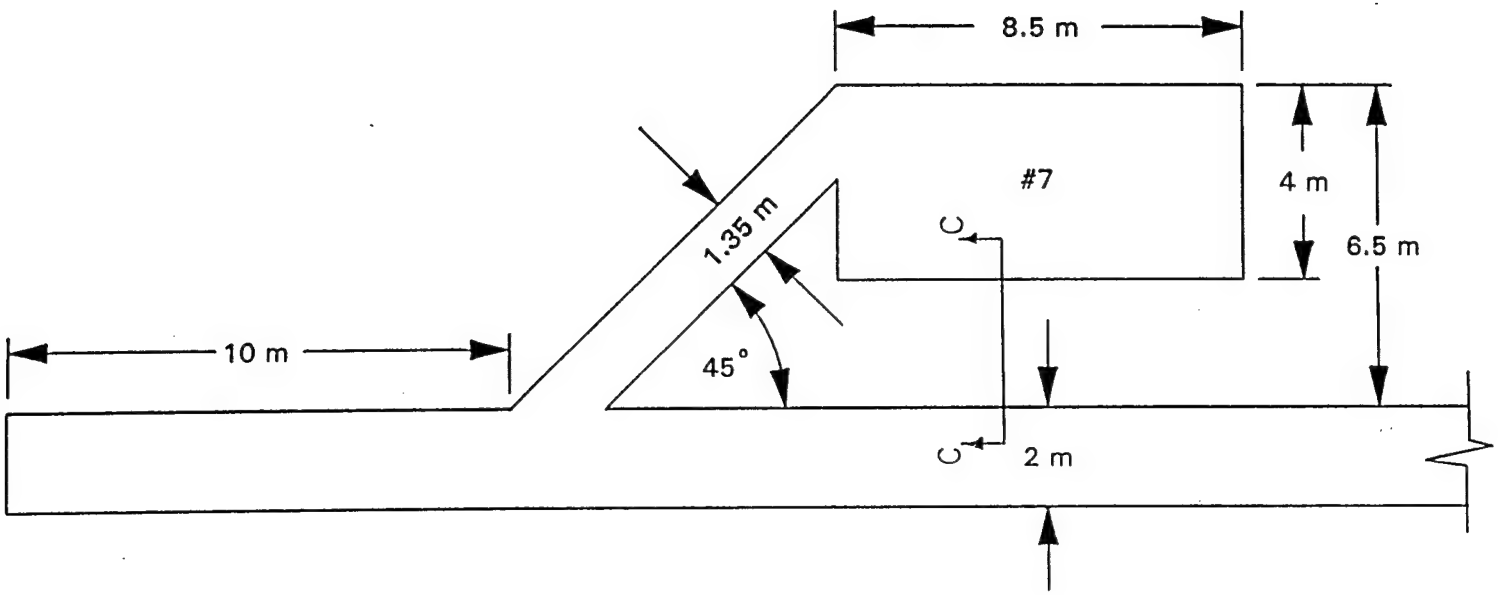

Figure 15. Plan view of Chamber 7.

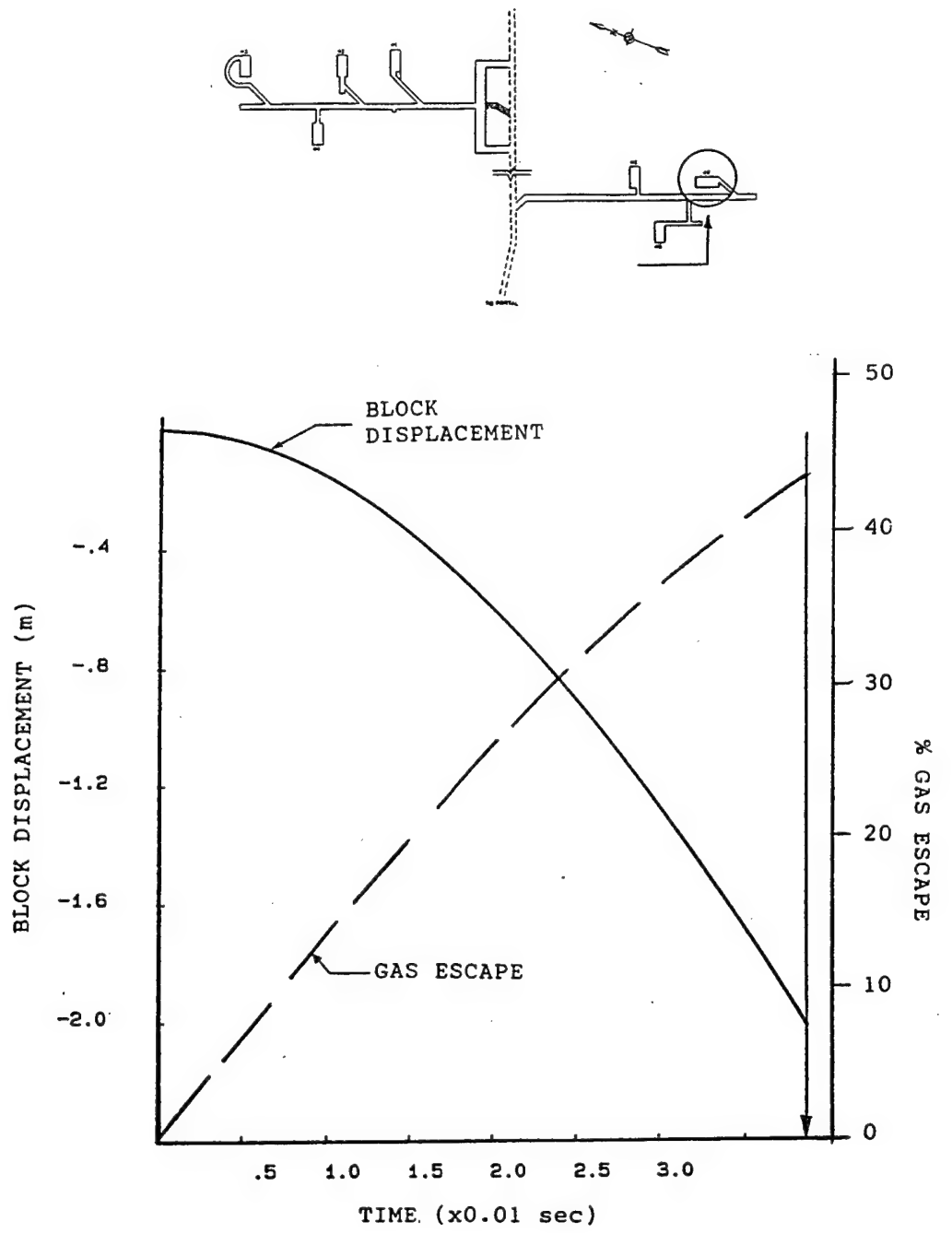

Figure 16. Displacement of the weak wall in Chamber 7 (along section C-C of Figure 15) and mass flow rate out of chamber.

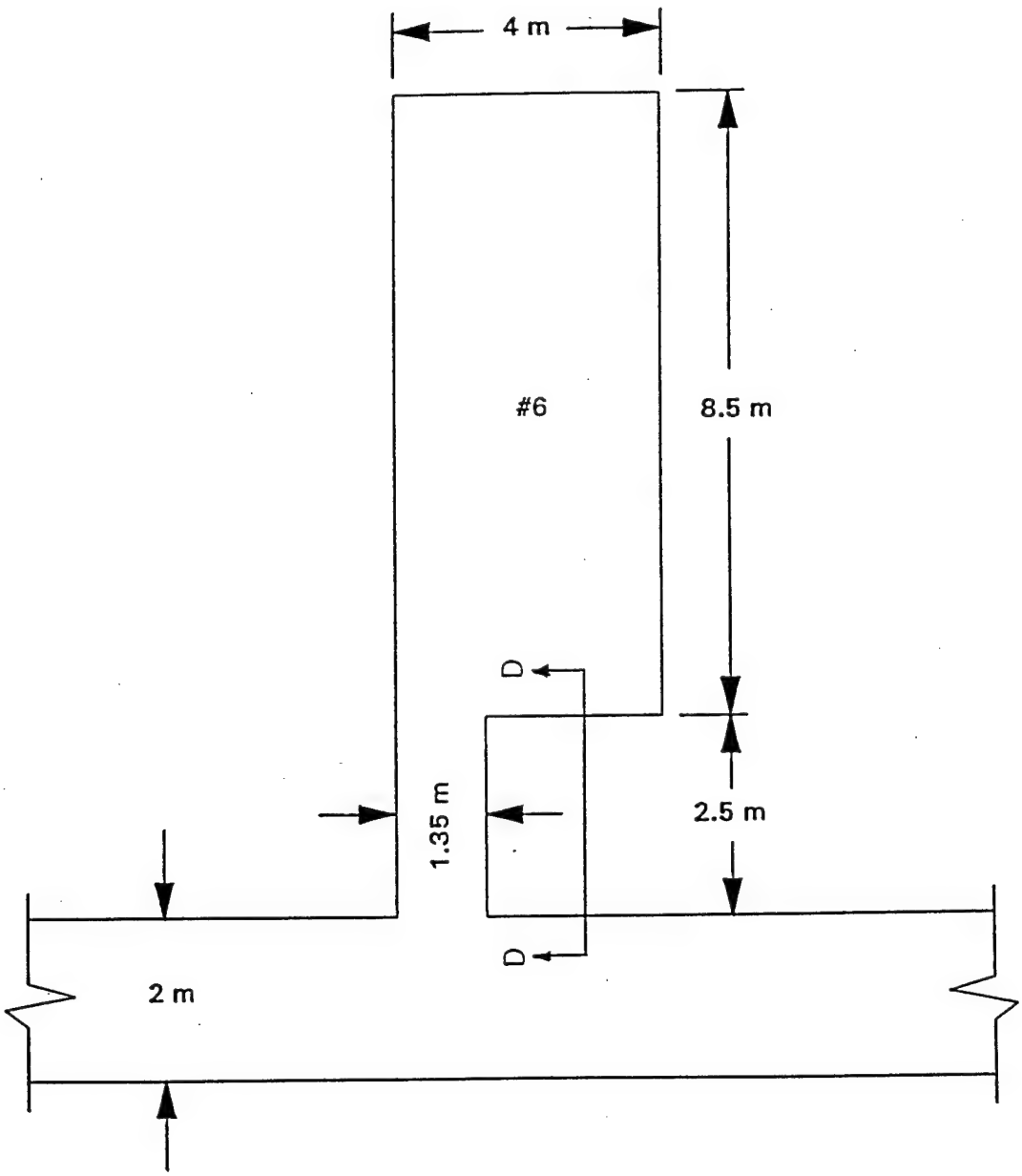

Figure 17. Plan view of Chamber 6.

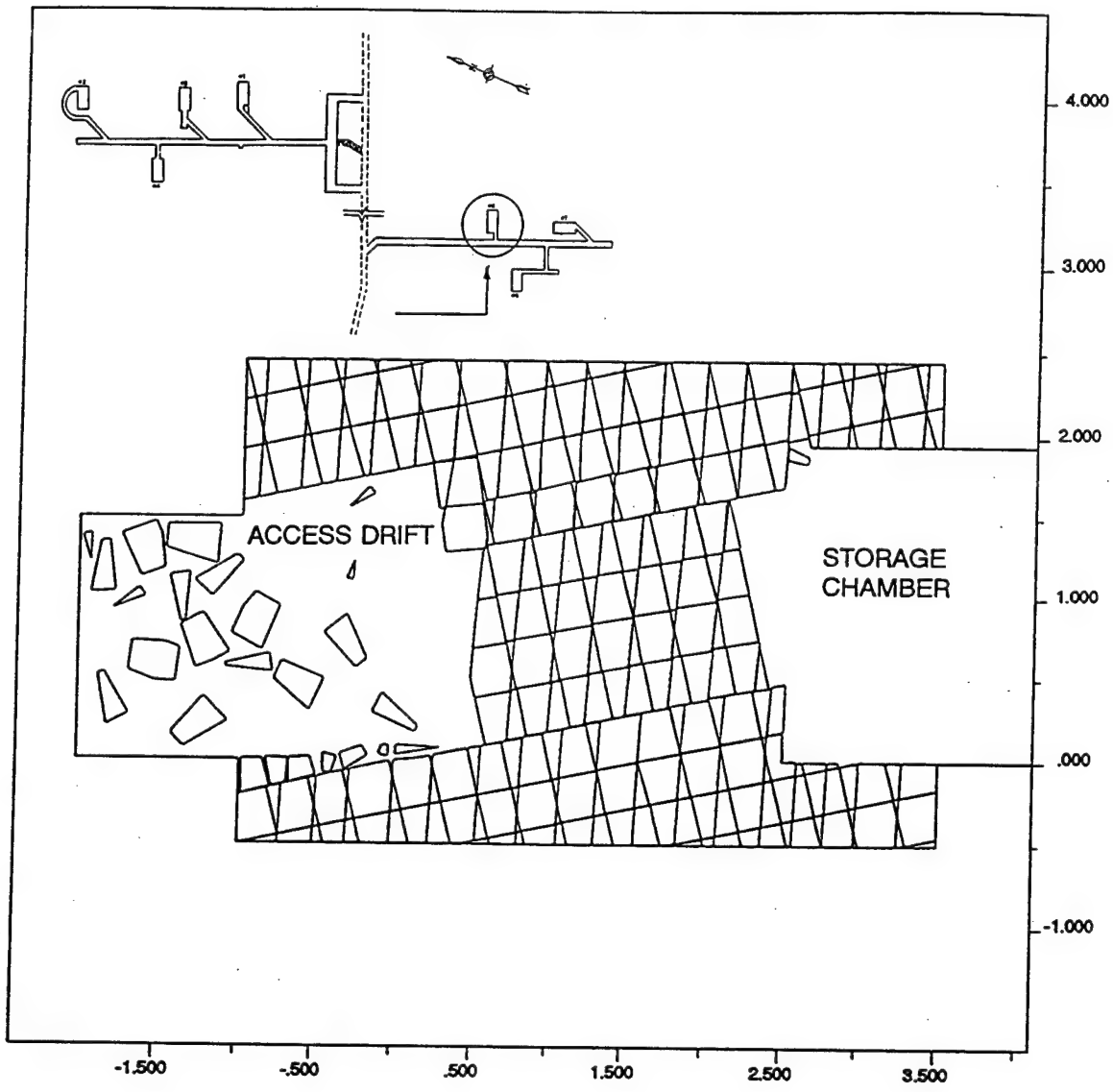

Figure 18. Spalling along Chamber 6 during the dynamic event (along section D-D of Figure 17).

4.2 Discussion of Results

The self-seal scenarios modeled included a sliding block (Chamber 1), a weakwall exhaust drift (Chamber 3), and a plain weak wall (Chamber 7). In addition, the stability of a portal between a chamber and the access drift during the dynamic event was modeled (Chamber 6).

An important observation made during the modeling process was that the sliding block and the weak walls moved under the dynamic load as solid blocks (shown in Figure 9 for Chamber 1). This observation has to be treated with great skepticism in that the solid behavior can change drastically to a rock-burst type of behavior where blocks of rock eject into the access drift and may be carried away by the rapid flow of hot gases out of the chamber. Under this circumstance, the mission of the self-seal plug is defeated, and additional hazards may be created due to flying debris. The change from solid block behavior to flying ejecta may be triggered by popping out of one or two key blocks or by a more impulsive type of explosion. The popping out may happen if the joint orientation or properties deviate from that modeled by UDEC. Figure 19 shows the behavior of Chamber 3 under a more impulsive blast than that predicted for the 1/3 scale tests. The blast impulse for the 1/3 scale tests is expected to last up to tens of msec, whereas the impulse used for Figure 19 is over 5 msec.

Assuming that the joint configurations and the blast impulse are similar to those observed in the field, and are predicted by the thermodynamic model, one can compare Figures 10 and 14 and observe that the weak wall-exhaust drift concept performs better in preventing the hot gases from escaping the chamber in an explosion. The comparison indicates that only 10% of the gases escape from Chamber 3, whereas up to 30% of gases escape from Chamber 1. In addition, the gases escaping Chamber 3 will be cooler, and will be moving slower when they reach the main access drift than those from Chamber 1. This is due to a larger expansion of the gases from Chamber 3 into the exhaust drift. The cooler gas reduces the potential of sympathetic detonation in the adjacent chambers, and the lower gas velocities do not have the capability of carrying ejecta for long distances.

The wall between Chamber 6 and the access drift was analyzed as a pillar without any pre-cut slots for weakening. This was done to determine the stability of the wall during the dynamic event. As shown in Figure 18, major spalling may occur on the access drift side of the pillar. The spall fragments may be caught in the hot gas stream and carried away into the adjacent chambers or to the portal. With further UDEC modeling and stability analysis, it is possible to design the wall thickness or support systems for the wall so that it can withstand the blast pressure without major spalling. Note that the spalling shown in Figure 18 may happen around the weak walls of Chambers 3, and 7.

Chamber 7 was modeled as a weak wall alone. From Figure 16 it is observed that up to 45% of the hot gases escape the chamber before complete closure. However, the gases escaping the chamber have to flow into the main access drift before reaching the location of closure. This will slow down the escape of gases around the weak wall. The exact quantity of this gas flow can be determined with further thermodynamic (blowdown) analysis.

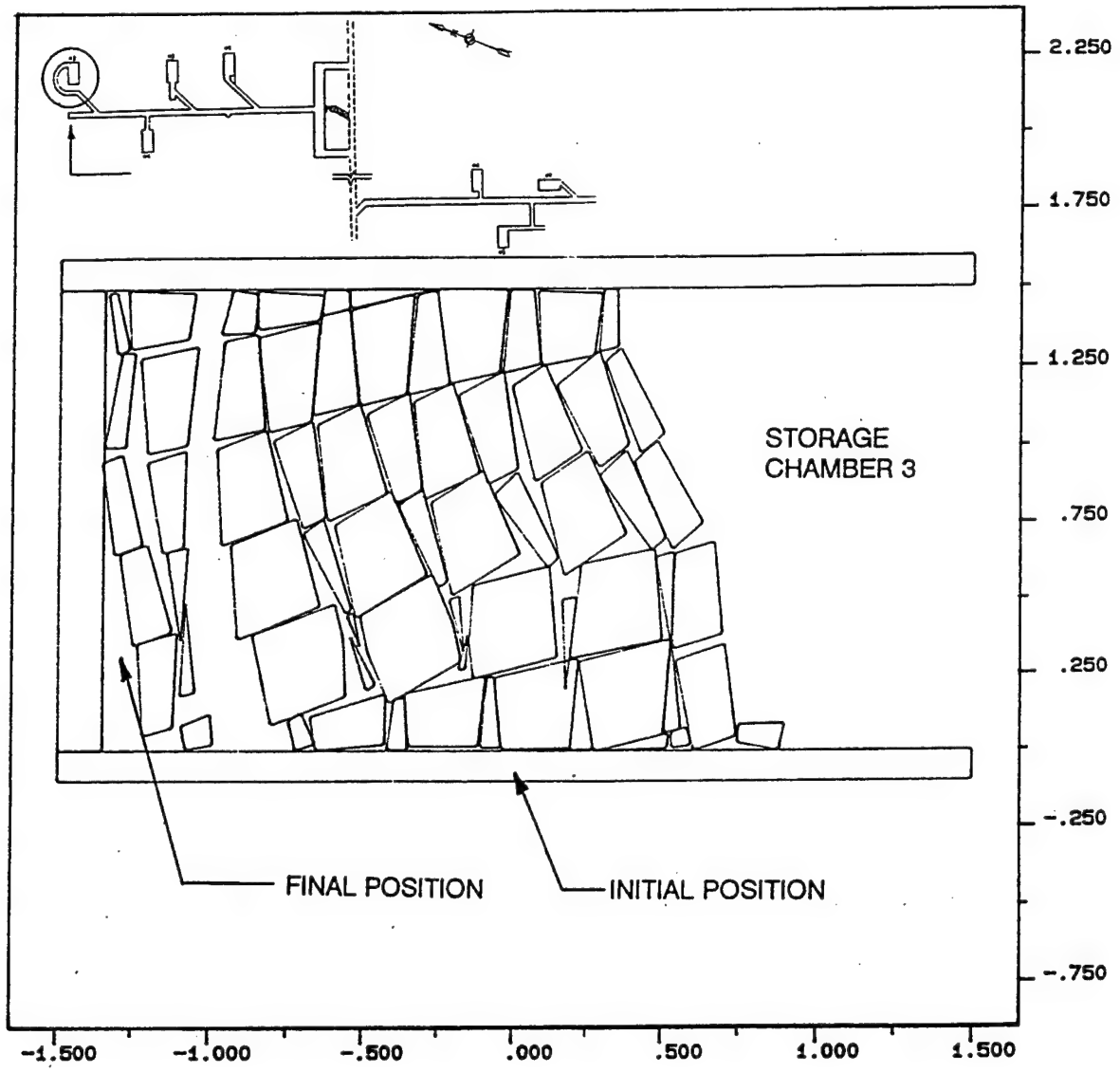

Figure 19. Spalling of Chamber 3, under a blast impulse of 5 msec duration.

5.0 ALTERNATIVE SELF-SEALING SYSTEM

There are several shortcomings associated with the weak wall and sliding block concepts modeled in Section 4, namely:

- slow reaction time leading to the escape of a large quantity of gas;
- flow of hazardous rock debris and ejecta into the access tunnel, and possible transport to other chambers or portal;
- difficult access and re-entry and reconstruction after an accidental explosion;
- less reliable performance due to variations in joints and rock mass properties.

A sliding blast door can be designed to overcome the shortcomings listed above. First, because of its lighter weight compared to solid rock blocks, it will have a faster reaction time leading to confinement of a larger volume of gas. Second, the blast door will remain intact under the blast pressures so that no debris will be thrown into the access tunnels. Third, the blast door can be slid open after the blast, providing immediate access to the storage chamber. Finally, the blast door can be designed and tested with reliable and predictable performance.

The concept is shown in Figure 20. Figure 21 shows details of the blast door which is configured to support maximum differential pressure for minimum blast door weight. As shown in the figure, the boiling chambers are initially filled with water, but during the explosion the water starts boiling, and removes some heat away from the aluminum door. The boiling chambers can be designed in such a way that the door temperature stays below the temperature at which aluminum loses too much of its strength. Steel could also be used.

The concept shown in Figure 20 has an approximate mass of 7500 lbm. Under the pressures expected in Chamber 1 during an accidental explosion, the door will completely seal the chamber in 16.5 msec. Over this period of time only 10% of the gases escape, whereas in the sliding block concept for Chamber 1, up to 30% of the gases escapes.

6.0 SUMMARY AND RECOMMENDATIONS

6.1 Summary

In this report, a coherent method for modeling of self-sealing systems for underground munitions storage facilities is presented. This method illustrated that observations made during field investigation can be incorporated into simulation models for realistic prediction of the behavior of storage chambers during an accidental explosion. The modeling approach incorporated a thermodynamic/numeric technique using a thermodynamic model developed by the UTD staff and a distinct element numerical code (UDEC) developed by Itasca Consulting Group, Inc.

Three self-seal scenarios were modeled. They included a sliding block, a weak wall exhaust drift, and a single weak wall. The performance of the weak wall exhaust concept was found to be superior to the sliding block and the weak wall concepts. This was due to a much smaller amount of hot gases that were predicted to escape through the weak wall exhaust system.

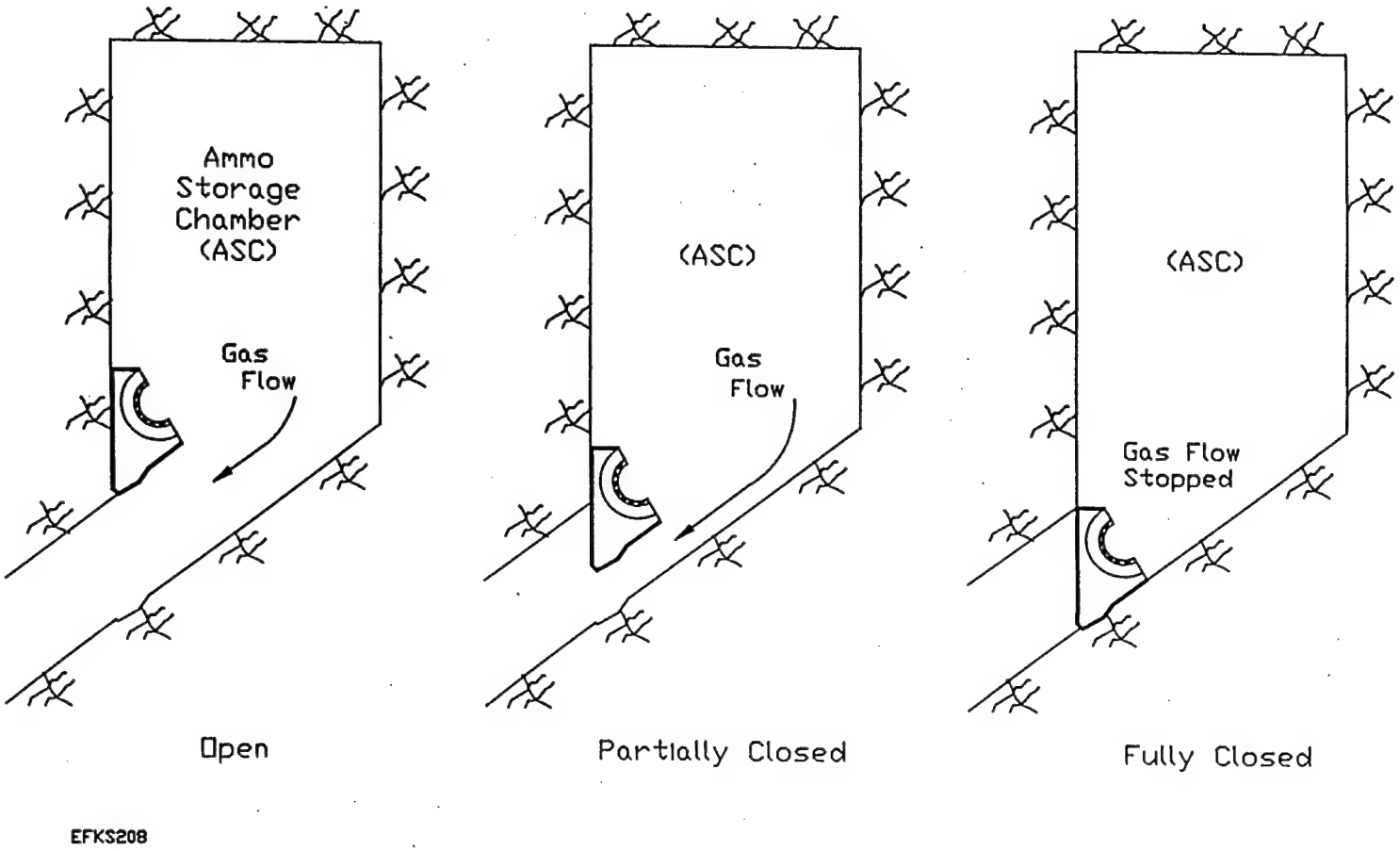

Figure 20. Operation of a proposed blast door concept during emergency closure.

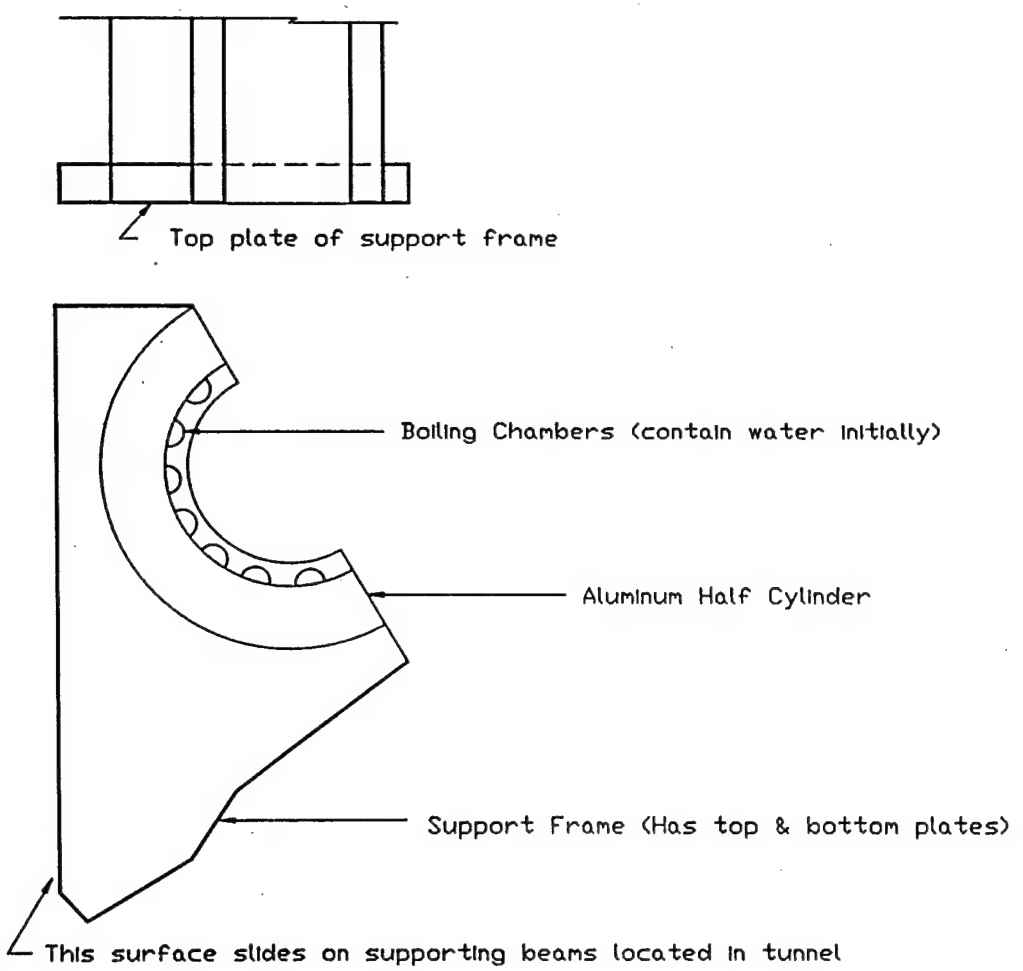

Figure 21. Schematic arrangement of the proposed blast door.

Because of the variability in jointing pattern, properties of the joints around the storage chambers, and possible short-period blast pressures, several shortcomings associated with the self-seal scenarios were identified. Chief among them was the possibility of the removal of key blocks into access drifts which may result in large-scale spalling into the access drifts. To overcome these shortcomings, a concept for an alternative self-seal system was developed. This consists of a specially designed blast door that can withstand the temperature and pressure of the hot gases inside the chamber, and be driven shut very rapidly by the blast pressure.

6.2 Recommendations

The models developed in this project require calibration before they are used for the analysis and design of full-scale storage chambers. The calibration can be carried out by measurements made during the construction phase of the 1/3 scale storage chambers, the dynamic event, inspection of the test site, and field measurements after the event. The measurements made during construction may be the convergence of access drift and chamber walls due to excavation. These measurements will be used in UDEC models of the excavation process to develop a methodology that relates field-measured convergence to joint properties. This methodology can then be used with field-measured convergence data during the excavation phase of the full-scale model in order to predict realistic joint properties for the full-scale test site.

Measurements made during the dynamic event will be mainly of the gas pressure, time of arrival, and blast impulse at various locations in the drifts and chambers. These measurements can be used to calibrate the thermodynamic model developed under this contract. The observations and measurements made during and after the dynamic event will be used to calibrate the UDEC modeling of the dynamic event. The joint properties determined from laboratory tests or through empirical methods are suited for stability analyses under excavation or mining conditions. These are relatively slow processes compared to blast loading during an accidental explosion. Under this kind of dynamic loading the joints will behave differently, and the measurements of wall movements made during the event may be used in calibrating the joint properties or developing models for their behavior.

7.0 REFERENCES

[1] UDEC, Version 1.8, ITASCA Consulting Group Inc., June 1992.

[2] Bieniawski, Z.T., ENGINEERING ROCK MASS CLASSIFICATIONS, Wiley Intersciences, 1989.

[3] Afrouz, A.A., PRACTICAL HANDBOOK OF ROCKMASS CLASSIFICATION SYSTEMS AND MODES OF GROUND FAILURE, CRC Press, 1992.

[4] Ibid, pp. 50-51.

[5] CONWEP Conventional Weapons Effects computer program based on TM 5 -885 -1, "Fundamentals of Protective Design for Conventional Weapons"; HQ, Dept. of the Army, Washington, D.C., 1986.

APPENDIX A

GEOTECHNICAL REPORT

ON SECTIONS OF THE

LINCHBURG MINE

A.1.0 INTRODUCTION

The following sections summarize the results of a field investigation of the U.S. Army Engineer Waterways Experiment Station's (WES) Intermediate-Scale Tunnel Test Site at the Linchburg Mine in the Magdalena Mountains, Socorro County, New Mexico, conducted in March 1993 by UTD, Inc. Figure A.1 is a location map of the test area. The objective of the investigation was to perform geologic mapping and to characterize the rock mass quality for subsequent prediction analysis of rock/tunnel/chamber response under explosive loading test conditions. The data that resulted from the geotechnical investigation were used to classify the rock mass according to the Rock Mass Rating (RMR) and Q systems and used as input to the UDEC computer model for the response analysis.

A.2.0 SITE DESCRIPTION AND GENERAL GEOLOGY

The Linchburg Mine is one of a number of fairly extensive lead -zinc mines in the Magdalena mining district and is located about 5 miles south of Magdalena, New Mexico. Figure A.2 (modified from WES "Preliminary" dated 3/17/93) is a generalized geologic map and shows the plan outline of the proposed excavations. Figure A.3 is a geologic cross-section taken along the portal drift and was constructed from the measurements made during the investigation, as well as from data from WES. The mountains are essentially a north-south trending "fault block structural exposure typical of this region of the Basin and Range Province, located near the southern edge of the Colorado Plateau and along the western margin of the Rio Grande Rift. Total relief in the region is of the order of 3000-3500 feet, with the mine portal about half-way up the west slope of the mountains at an elevation of 8050 feet.

The Linchburg Mine has several thousand feet of underground workings. Mineralization is associated with the Linchburg fault and related fault/fracture systems where Paleozoic limestones are in fault contact with the Precambrian core complex which forms the spine of the Magdalena Mountains. From the mine portal, the existing mine drift penetrates about 300 feet of Tertiary volcanics, then approximately the same amount of Madera Limestone (and shale) and then the balance of the length of the drift is within the Kelly Limestone. The actual stratigraphic thickness of the Kelly is about 125 feet in the vicinity of the Linchburg Mine. The rock here is a dense, coarsely crystalline limestone with some fossils, chert nodules and more pure calcite stringers present. All of the sedimentary units strike generally to the north and dip gently west about 8-20 degrees. In both structural regions there are basically two dominant joint sets with steep dips (70 degrees to near vertical). The strike of the joints is generally within 50 degrees east and west of north. (Note: In the text and on the RMR data sheets, all azimuths are magnetic as measured. These data have been translated into grid azimuths for plotting on maps using the grid-magnetic declination of 11.5°E. Cross-sections were prepared by converting true dips to apparent dips to produce accurate look direction geometries.)

The portal drift parallels and roughly corresponds to the axis of a fairly broad anticline reported by Titley (1957, 1961). The anticline, and its attendant smaller scale folding, intersects

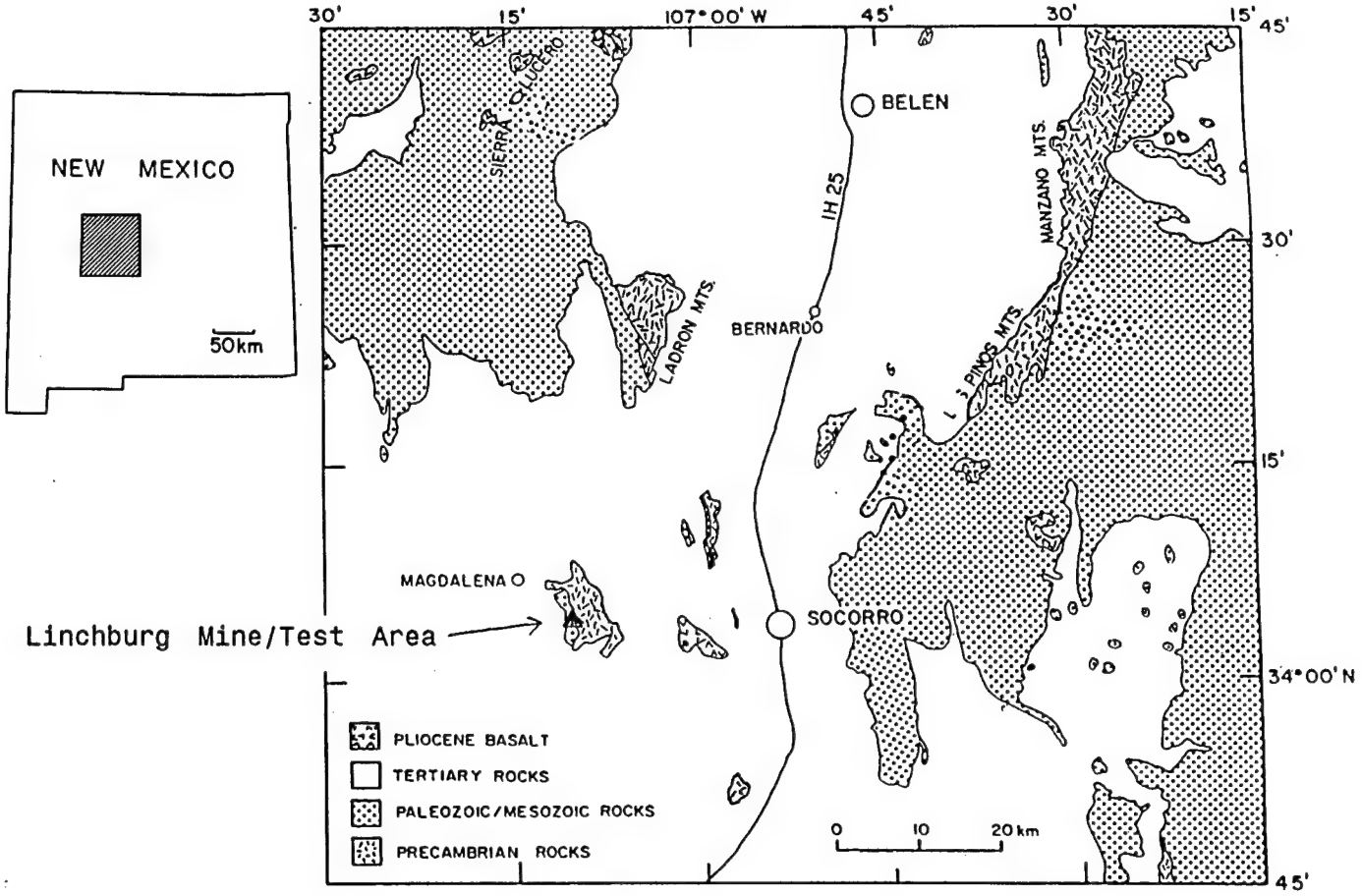

Figure A.1. Location Map of the Linchburg Mine/Test Area with generalized geology.

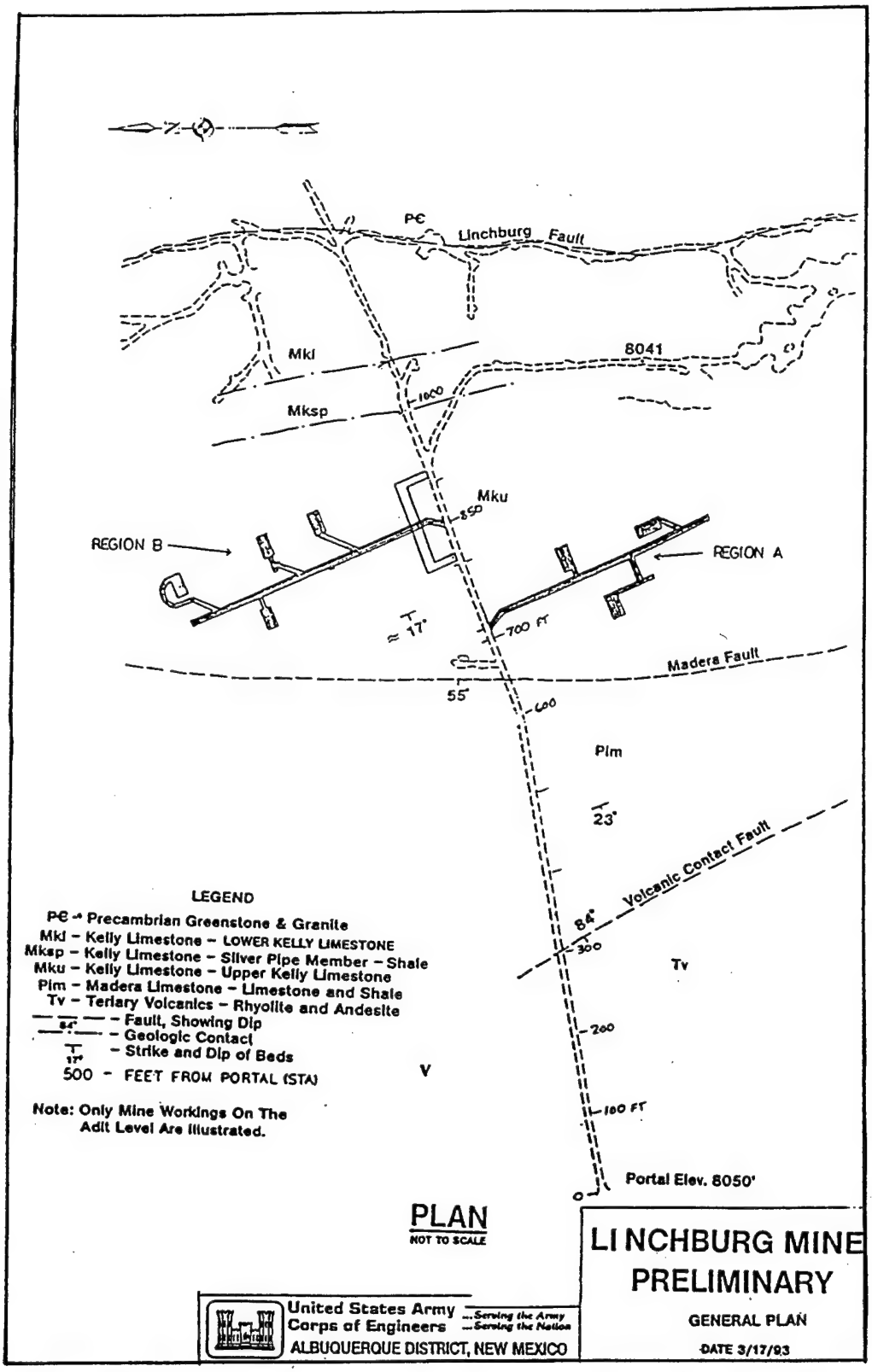

Figure A.2. General geologic map of the Linchburg Mine - Scaled Test Site (modified from COE Preliminary Map).

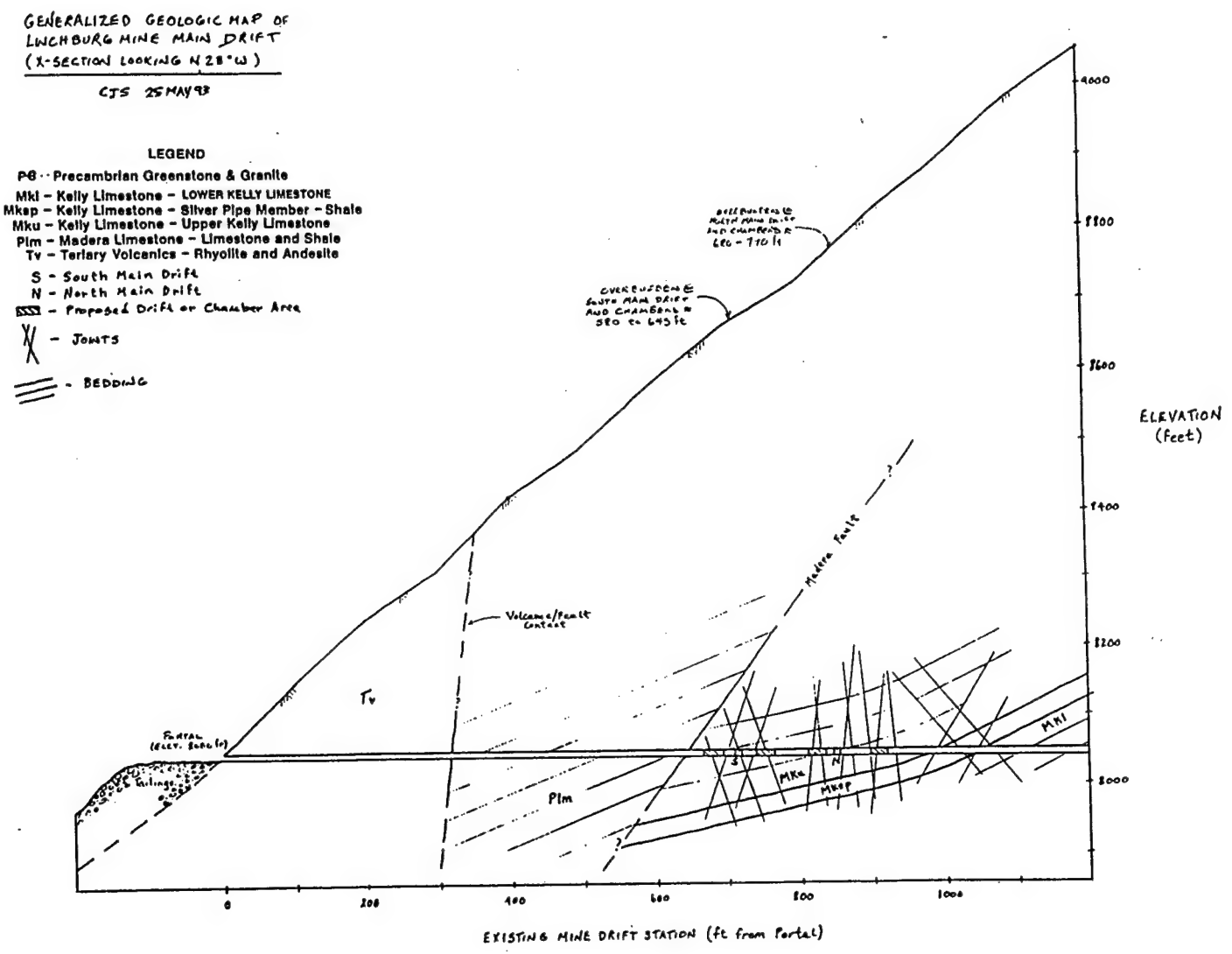

Figure A.3. Generalized geologic cross-section taken along the main portal drift.

(and is approximately perpendicular to) the major fault systems and the northerly-trending mountains. The anticline is of low amplitude and plunges gently to the west.

A.3.0 DETAILED GEOLOGYAND GEOMECHANICAL CLASSIFICATION

The two main drifts to the chambers will be excavated so as to be perpendicular to the existing portal drift; one exiting to the south and one to the north. The South Test Drift and chambers are located adjacent to portal drift Station 700 (700 feet into the mine from the portal) and the North Test Drift and chambers at Station 850. While both chamber groupings will be excavated in the Upper Kelly Limestone, their spatial separation conveniently leads to individual analysis and classification of the two local rock masses. We will term these Structural Region A (along the South Test Drift) and Structural Region B (along the North Test Drift).

Since none of the test drifts or chambers had been excavated, this study relies on geologic mapping of rock exposed at the existing mine workings and a review of the existing literature. Extrapolation of these data to characterize the rock mass at the test chambers seems warranted given the relatively minor lithologic and structural variations observed locally (the rock exposed in the mine portal drift between Station 700 and 850) and the documented tendency for these strata to be fairly homogeneous laterally.

An exception to this would be the observed vuggy zones and small solution cavities within the limestone, often aligned along joints and fractures. While these are anticipated to be of limited extent in the chambered rock mass, it is possible that excavation will intercept a zone of increased solutioning (and perhaps mineralization) in this type of rock, and therefore a zone of differing rock mass quality. Additionally, if the portal drift essentially follows the anticlinal axis, it can be expected that the chambers excavated to the south (Region A) will be developed on the southern limb of the fold while the north chambers (Region B) will fall on the northern limb. Given the broad nature of the anticline (about 70 ft of vertical change in a lateral distance of about 850 ft) this variance should result only in a small variance of the local bedding dip (perhaps 2-5 degrees from fold crest to extent of limb) and dip direction.

The site investigation revealed no significant variation in lithology from Region A to B. In the absence of any laboratory analyses of the host limestones, the rock was estimated to be of medium high to high strength (about 100 MPa or 14500 PSI or greater, typical of average limestones) and the RQD is in the 75-90% range, indicative of "good" quality.

A.3.1 Structural Region A

Structural Region A characterization is intended to be representative of the rock at Chambers 5, 6, and 7 and associated drifts. Table A.1 is a completed Geomechanics Classification data form which summarizes the geologic and structural data for the rock of Region A.

The Upper Kelly Limestone beds are undulatory and dips range from 10-14 degrees W -SW to S with strikes varying from N55°W to N75°E. They form a stepped appearance when looking

Table A.1. Region A (South Chambers) rock mass data.

INPUT DATA FORM : GEOMECHANICS CLASSIFICATION (ROCK MASS RATING SYSTEM)

Name of project: WES - LINCHBURG (STA 650-750 ft)
Site of survey: STA ~ 700
Conducted by: UTD
Date: MAR 1993

STRUCTURAL REGION	DEPTH, m	ROCK TYPE
A	190 m	LIMESTONE

STRENGTH OF INTACT ROCK MATERIAL

Designation	Uniaxial compressive strength, MPa	OR	Point-load strength index, MPa
Very High:	Over 250		>10
High:	100-250	✓	4-10
Medium High:	50-100	X	0-4
Moderate:	25-50		1-2
Low:	5-25		<1
Very Low:	1-5		

DRILL CORE QUALITY R.Q.D.

Excellent quality:	90-100%	
Good quality:	75-90%	✓
Fair quality:	50-75%	
Poor quality:	25-50%	
Very poor quality:	<25%	

R.Q.D. = Rock Quality Designation

STRIKE AND DIP ORIENTATIONS

	Strike	(from ... to ...)	Dip: (angle)	(direction)
Set 1 BEDDING	N 25° W (average)	(from N 75° E to N 55° W)	13°	SW-W
Set 2 JOINT #1	N 35° E	(from N 19° E to N 38° E)	71-85°	NW
Set 3 JOINT #2	N 58° W	(from N 55° W to N 60° W)	75°	NE
Set 4		(from ... to ...)		

NOTE: Refer all directions to magnetic north. ✓

SPACING OF DISCONTINUITIES

		Set 1	Set 2	Set 3	Set 4
Very wide:	Over 2 m				
Wide	0.6 - 2 m				
Moderate:	200 - 600 mm	✓	✓	✓	
Close:	60 - 200 mm				
Very close:	< 60 mm				

GROUND WATER

INFLOW per 10 m of tunnel length: ..... liters/minute
or
WATER PRESSURE ..... kPa

GENERAL CONDITIONS: completely dry, / damp / wet, dripping or flowing under low/medium or high pressure): STA. 725

IN SITU STRESSES

CONDITION OF DISCONTINUITIES

		Set 1	Set 2	Set 3	Set 4
PERSISTENCE (CONTINUITY)					
Very low:	< 1 m				
Low:	1 - 3 m				
Medium:	3 - 10 m		✓	✓	
High:	10 - 20 m				
Very high:	> 20 m	✓			
SEPARATION (APERTURE)					
Very tight joints:	< 0.1 mm	✓	✓	✓	
Tight joints:	0.1 - 0.5 mm	✓			
Moderately open joints:	0.5 - 2.5 mm				
Open joints:	2.5 - 10 mm				
Very wide aperture:	> 10 mm				
ROUGHNESS (state also if surfaces are stepped, undulating or planar)					
Very rough surfaces:					
Rough surfaces:		✓			
Slightly rough surfaces:		✓	✓	✓	
Smooth surfaces:					
Slickensided surfaces:					
FILLING (GOUGE)					
Type:		(trace)	clay/calcite	calcite	calcite
Thickness:		trace to:	1-2 mm	1-2 mm	1-2 mm
Uniaxial compressive strength, MPa		N/A			
Seepage:		DRY to trace dampness			
WALL ROCK OF DISCONTINUITIES					
Unweathered		✓	✓	✓	
Slightly weathered		✓	✓	✓	
Moderately weathered		✓			
Highly weathered					
Completely weathered					
Residual soil					

GENERAL REMARKS AND ADDITIONAL DATA

MAJOR FAULTS specify locality, nature and orientations.
Madera Fault @ Sta 625 - 635 (ft), strikes NORTH, dips ≈ 55° W; 1-2 gpm flowing water.

NOTE: For definitions and methods consult ISRM document: *'Quantitative description of discontinuities in rock masses.'*

"east" because of their regular spacing and low angle of dip. The primary joint set strikes N19-38°E and dips 71-85 degrees to the northwest. Joint Set #2 strikes from N55-60°W with a fairly consistent dip of about 15 degrees NE. A tertiary and subordinate set of joints was measured to strike N12-25°E with somewhat more shallow angled dips in the 56-71°NW range. Figure A.4 is a plan view of Structural Region A with the structural geologic information placed approximately where measured along the portal drift (and along an adit which is about 275 feet NE of Chamber #6). Spacing of the bedding planes and the two main joint sets is remarkably similar and falls within the moderate category at 8 to 16 inches (200 to 400 mm) spacing, although some closer and wider spacing was observed. The third set has widely spaced joints in the 2 to 4 foot (0.6 to 1.2 m) range. Figure A.5 is a representative cross-section through the "south"-trending main drift and access drift given the above described jointing and bedding. Figure A.6 provides a generalized cross-section of the mapped structure about the portal drift opening (looking east).

The general condition of the wall rock at joint/bedding plane discontinuities is essentially unweathered to slightly weathered in the sense that they generally do not contain large amounts of clay or other alteration products in a disaggregated or gouge-like form. If the discontinuities have significant filling, it often is in the form of calcite mineralization, perhaps related to recrystallization or mineralization "healing" of the joints or bedding, planes. On the occasional joint or bedding planes which displayed some alteration, generally only a film of clay was observed on the discontinuity surface when broken apart. All of the joint discontinuities are highly persistent (10-20 m) and may be more continuous than can be estimated from existing exposures. The bedding planes have very high persistence (> 20 m). Most joint discontinuities are characterized as being tight (0.1-0.5 mm separation. Where bedding plane and joint surfaces were observed, they were slightly rough to rough, with bedding planes displaying greater roughness.

The rock between Stations 700 and 750 is generally dry with one exception being a damp/wet zone (no dripping or flowing water) at Station 125 which appears to be associated with a vuggy zone developed along one of the Set #2 joints. This may be an indication that there is some hydraulic communication with the Madera Fault which dips above and may come to within about 100-150 ft of the portal drift at Station 725. The north-trending Madera Fault (zone) intersects the portal drift at about Station 625-635 at a moderate dip of about 55°W. In this interval about 1-2 gallons per minute of water are flowing from the crown and along the drift walls.

Given the wet conditions along the fault and the presence of discontinuities and solution (vugs, cavities) features to provide the necessary conduits for hydraulic communication, it is possible that some moist or wet zones may be encountered upon chamber and drift excavation. Adding a significant amount of moisture to the chamber rock mass will tend to further reduce the RMR rating that is proposed on the basis of relatively dry conditions.

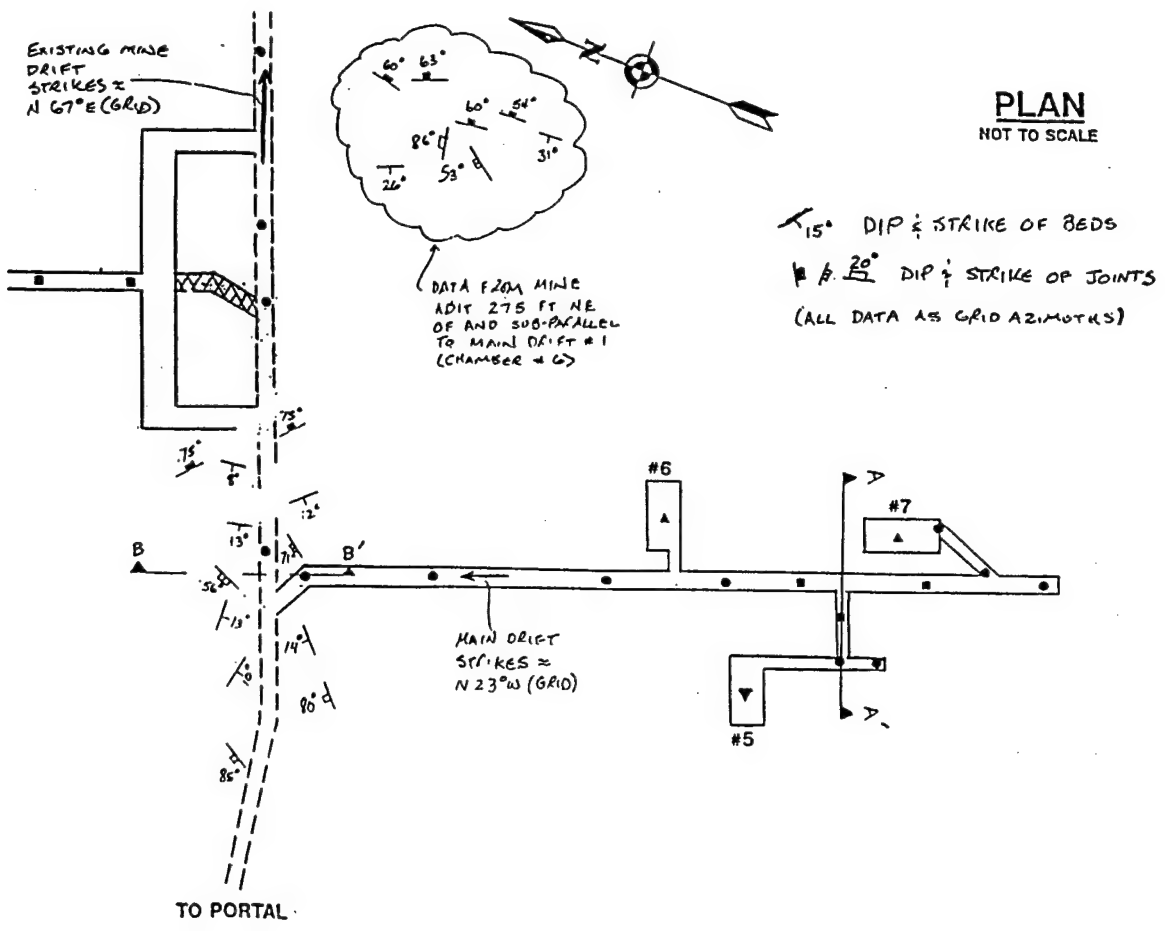

Figure A.4. Structural Region A (South Chambers) structural and geologic information - plan view.

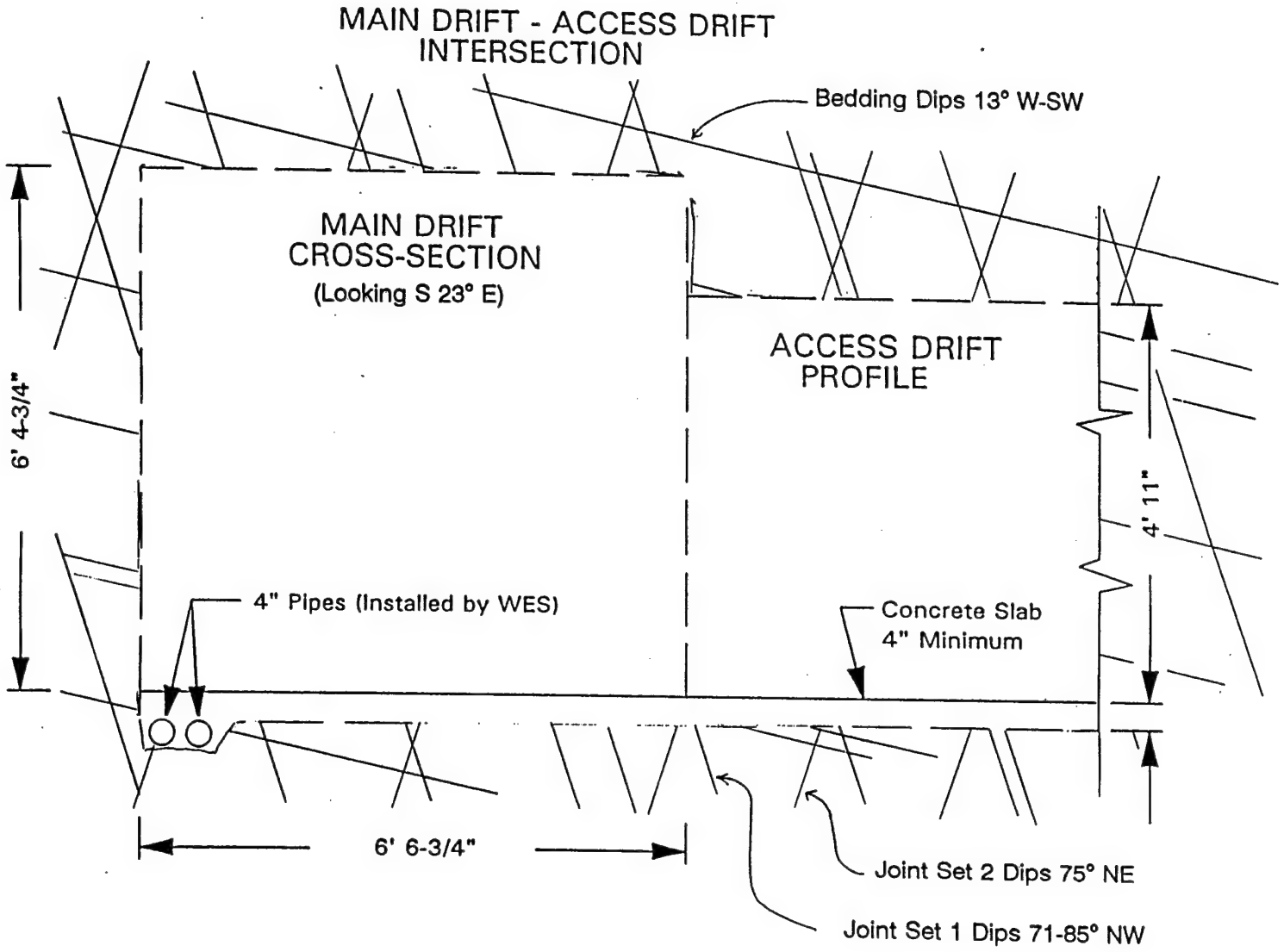

Figure A.5. Representative cross-section (A-A' from Figure A.4) showing structure in Region A - looking "south".

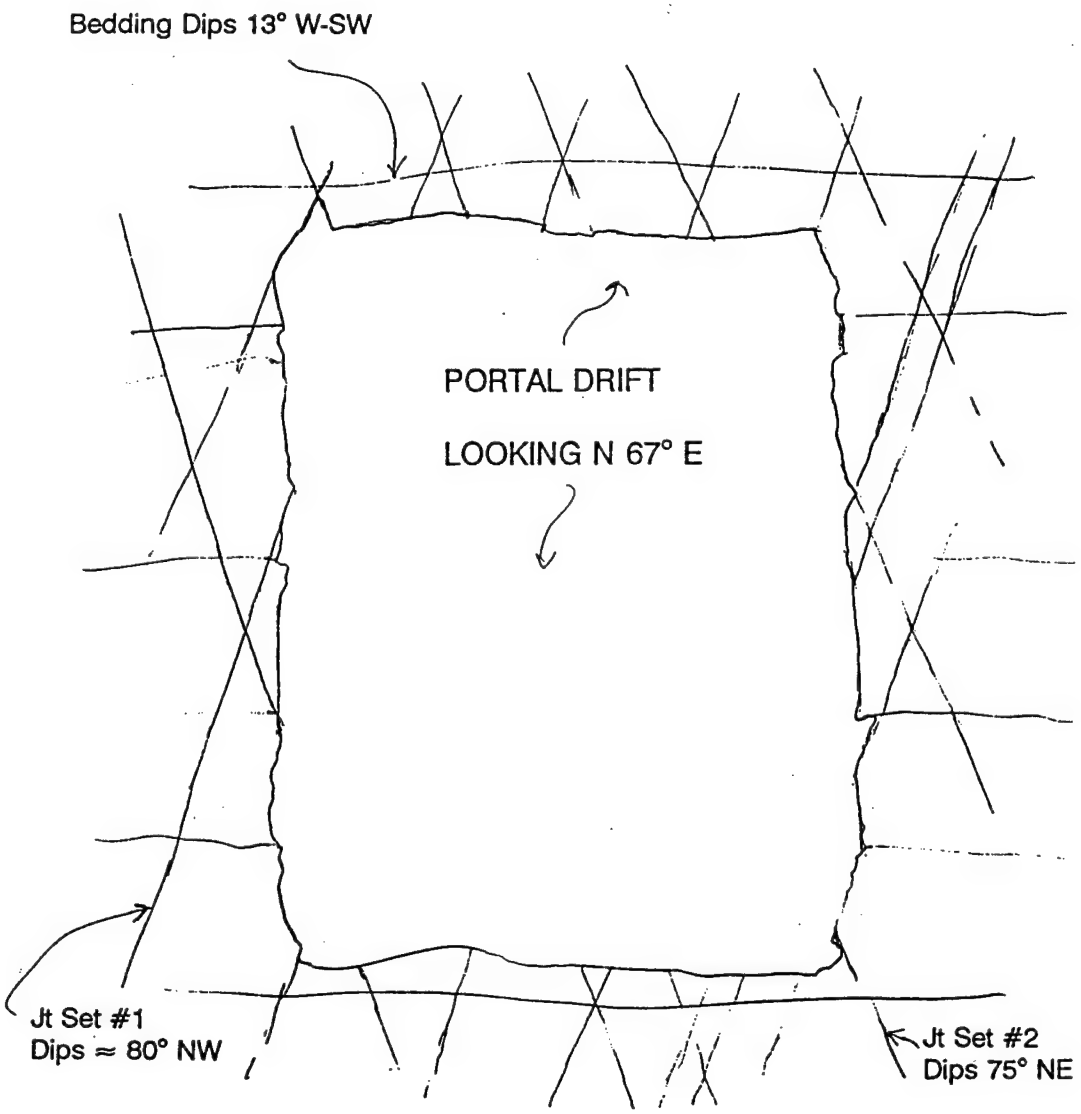

Figure A.6. Representative cross-section (B-B' from Figure A.4) showing structure in Region A - looking "east".

A.3.2 Structural Region B

Structural Region B relates to Chambers 1, 2, 3 and 4 and associated drifts. A completed Geomechanics Classification data form for this region is included as Table A.2 to provide a summary of pertinent geologic and structural information. Figure A.7 is a plan view of Structural Region B with data located approximately where measured.

Spacing, separation, persistence, filling material and roughness characteristics of the joints and bedding planes, along with the nature of wall rock (weathering) at Structural Area B, are all consistent with that presented for Area A. The section of portal drift located between Stations 800 and 850 is relatively dry, with only sporadic dampness observed. This may correlate with greater distance from the Madera Fault and greater overburden (about 750 feet compared with about 600 feet for Region A). Figure A.8 is a representative geologic/structural cross-section through the north-trending main drift at an intersection with an access drift. This section should be applicable for the rock mass surrounding Region B chambers, given a north look direction. Figure A.9 is a geologic cross-section through the main portal drift at Region B looking east. This section should be applicable to the structure surrounding the Region B chambers and access drifts given similar look directions.

A.4.0 SUMMARY

The rock mass surrounding the proposed Intermediate-Scale Tunnel Test chambers and related excavation is a relatively competent, coarsely crystalline and dense limestone which has been folded into a gently dipping and west plunging anticline structure. The limestone dips gently westward and is punctuated by three steeply dipping and moderately spaced joint sets. Discontinuities are generally highly persistent, tight, slightly rough to rough, unweathered or slightly weathered, and filling (gouge, etc.) is either minimal or as thin films of relatively dry clay material. The rock mass is generally dry to damp, with no flowing or seeping groundwater. The rock is quite uniform in bulk appearance and has only occasional chert nodules, calcite stringers, solution features (vugs and cavities) and other mineralized zones.

A.5.0 REFERENCES

Titley, S.R., 1957, "Structural and Mineralogical Control of Ore, Linchburg Mine, Socorro County, New Mexico," New Mexico Bureau of Mines and Min. Res., Open File Report, 11 pp.

Titley, S.R., 1961, "Genesis and Control of the Linchburg Orebody, Socorro County, New Mexico," Economic Geology, Vol. 56, No. 4, pp. 695 -722.

Table A.2. Region B (North Chambers) rock mass data.

INPUT DATA FORM : GEOMECHANICS CLASSIFICATION (ROCK MASS RATING SYSTEM)

Name of project: WES - LINCHBURG (STA. 800 - 875 Ft)

Site of survey:
Conducted by: UTP
Date: MARCH 1993

STRUCTURAL REGION	DEPTH, m	ROCK TYPE
B	220 m	LIMESTONE

STRENGTH OF INTACT ROCK MATERIAL

Designation	Uniaxial compressive strength, MPa	OR	Point-load strength index, MPa
Very High:	Over 250		>10
High:	100-250	✓	4-10
Medium High:	50-100	✓	0-4
Moderate:	25-50		1-2
Low:	5-25		<1
Very Low:	1-5		

DRILL CORE QUALITY R.Q.D.

Excellent quality:	90-100%	
Good quality:	75-90%	✓
Fair quality:	50-75%	
Poor quality:	25-50%	
Very poor quality:	< 25%	

R.Q.D. = Rock Quality Designation

STRIKE AND DIP ORIENTATIONS

BEDDING Set 1	Strike	N20°W	(from NORTH to N75°W)	Dip:	12°	W-SW
JOINT #1 Set 2	Strike (average)	N50°E	(from N47°E to N55°E)	Dip: (angle)	87°	(direction) NW/SE
JOINT #2 Set 3	Strike	N55°W	(from N50°W to N70°W)	Dip:	85°	E-NE
JOINT #3 Set 4	Strike	NORTH	(from N to N)	Dip:	77°	E

NOTE: Refer all directions to magnetic north.

SPACING OF DISCONTINUITIES

		Set 1	Set 2	Set 3	Set 4
Very wide:	Over 2 m				
Wide	0.6 - 2 m				✓
Moderate:	200 - 600 mm	✓	✓	✓	✓
Close:	60 - 200 mm				
Very close:	< 60 mm				

GROUND WATER

INFLOW per 10 m of tunnel length: liters/minute ..... or
WATER PRESSURE: kPa .....

GENERAL CONDITIONS (completely dry, slightly damp, wet, dripping or flowing under low/medium or high pressure):

IN SITU STRESSES

CONDITION OF DISCONTINUITIES

PERSISTENCE (CONTINUITY)		Set 1	Set 2	Set 3	Set 4
Very low:	< 1 m				
Low:	1 - 3 m				
Medium:	3 - 10 m				✓
High:	10 - 20 m		✓	✓	✓
Very high:	> 20 m	✓			
SEPARATION (APERTURE)					
Very tight joints:	< 0.1 mm				
Tight joints:	0.1 - 0.5 mm	✓	✓	✓	✓
Moderately open joints:	0.5 - 2.5 mm	✓			
Open joints:	2.5 - 10 mm				
Very wide aperture:	> 10 mm				
ROUGHNESS (state also if surfaces are stepped, undulating or planar)					
Very rough surfaces:					
Rough surfaces:		✓			
Slightly rough surfaces:		✓	✓	✓	✓
Smooth surfaces:					
Slickensided surfaces:					
FILLING (GOUGE)					
Type: (trace)		clay/cc	clay/cc	clay/cc	clay/cc
Thickness: trace to :		1-2mm	1-2mm	1-2mm	1-2mm
Uniaxial compressive strength, MPa		N/A			
Seepage:		NONE	→	→	→
WALL ROCK OF DISCONTINUITIES					
Unweathered		✓	✓	✓	✓
Slightly weathered		✓	✓	✓	✓
Moderately weathered					
Highly weathered					
Completely weathered					
Residual soil					

GENERAL REMARKS AND ADDITIONAL DATA

MAJOR FAULTS specify locality, nature and orientations.
MADERA FAULT 225 FT AWAY, SEE "A" FORM.

NOTE: For definitions and methods consult ISRM document: *'Quantitative description of discontinuities in rock masses.'*

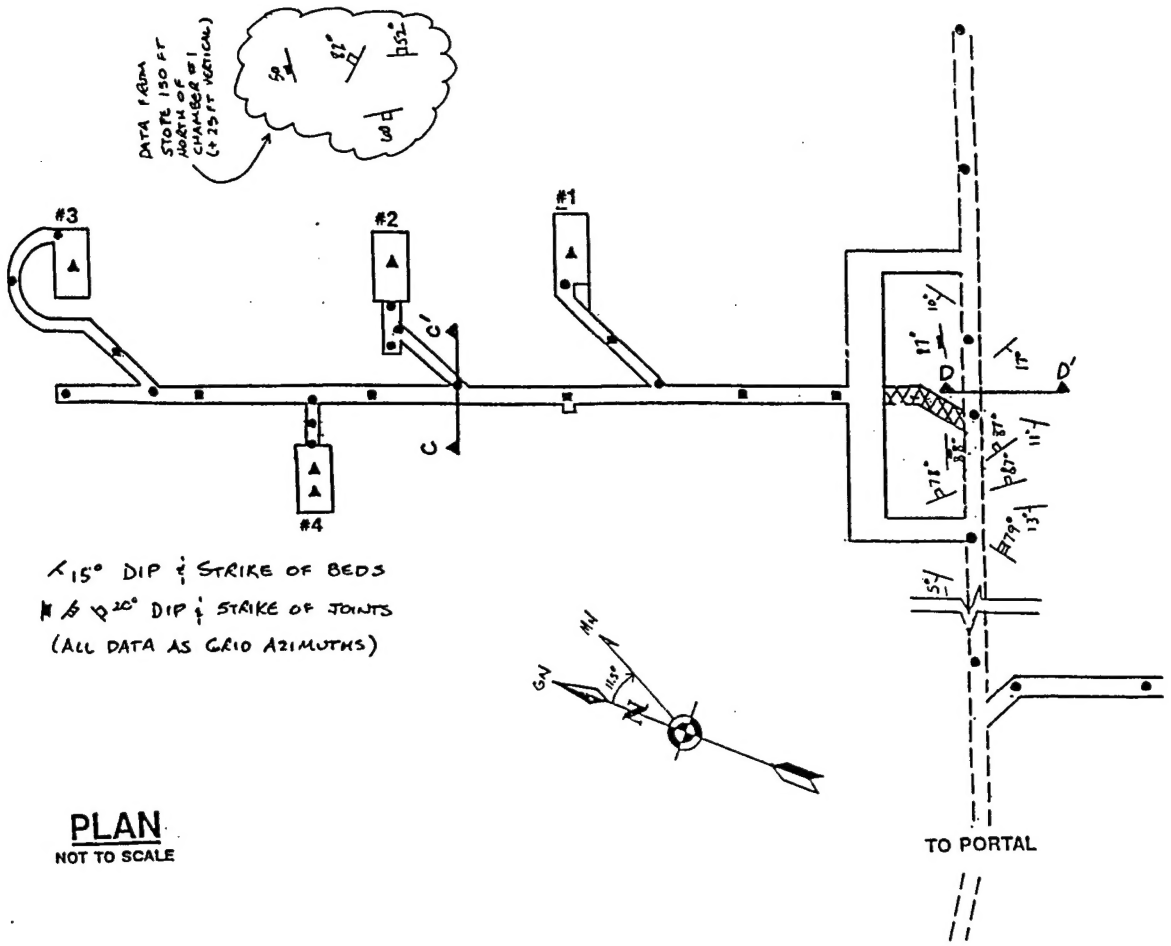

Figure A.7. Structural Region B (North Chambers) structural and geologic information - plan view.

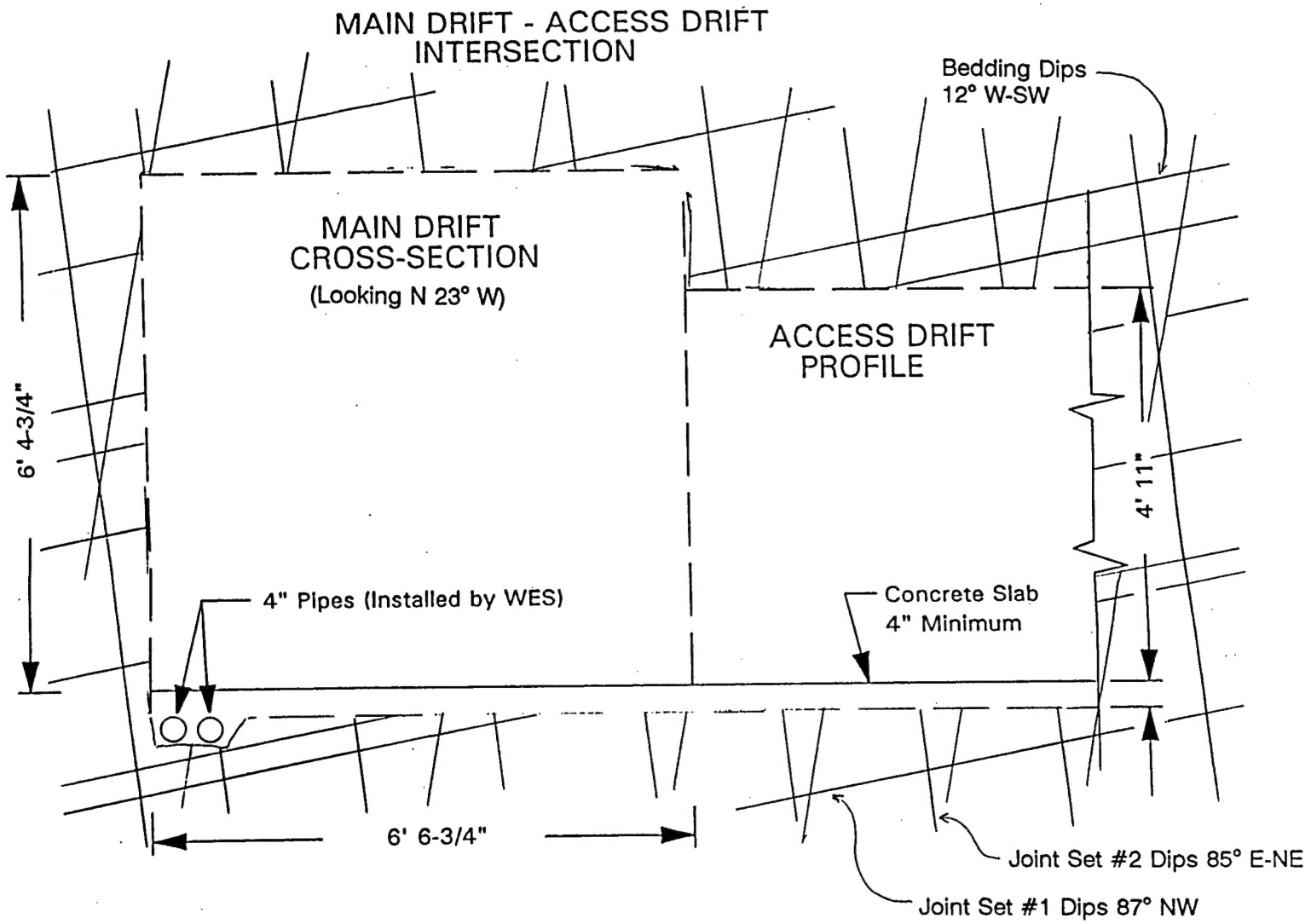

Figure A.8. Representative cross-section (C-C' from Figure A.7) showing structure in Region B - looking "north".

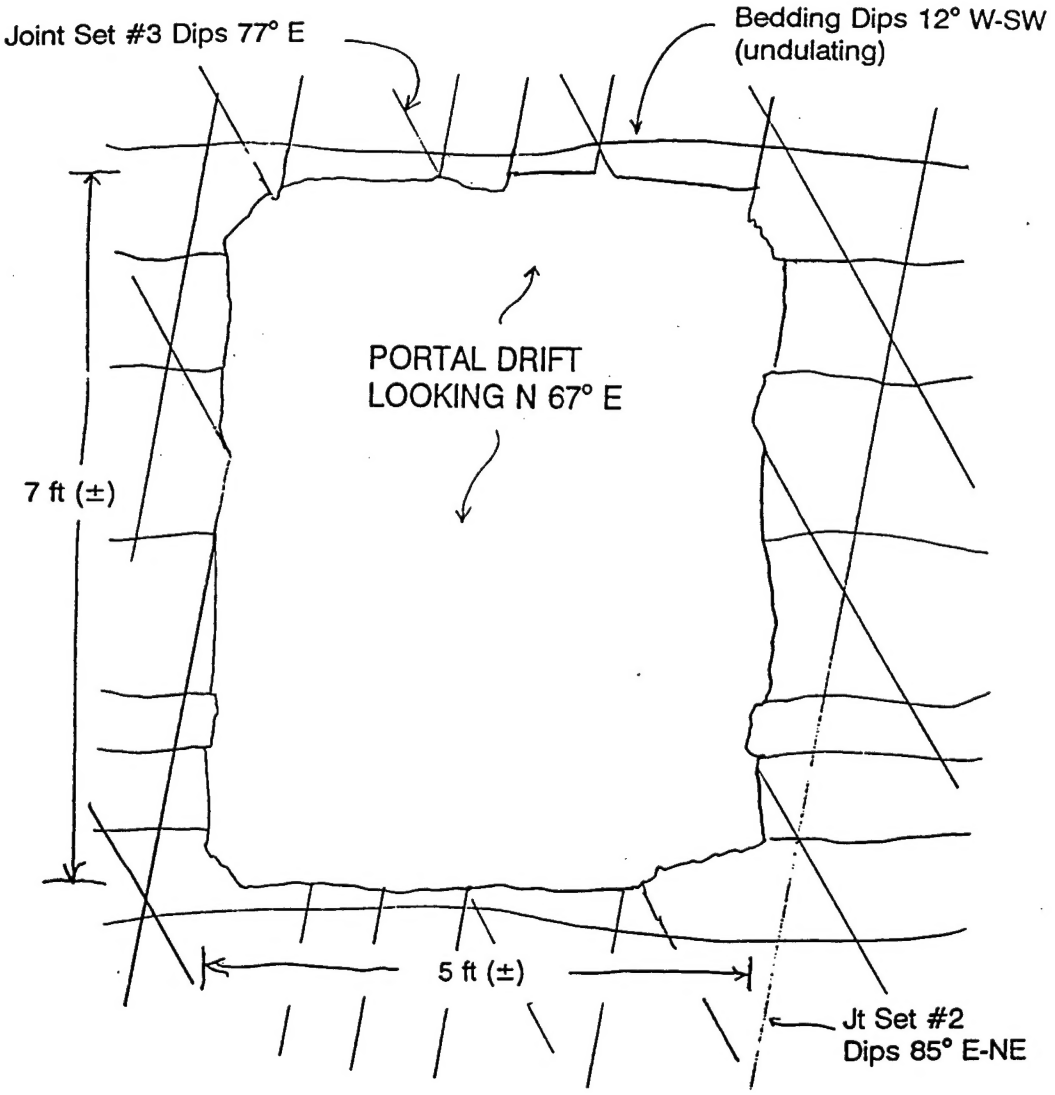

Figure A.9. Representative cross-section (D-D' from Figure A.7) showing structure in Region B - looking "east".

REPORT DOCUMENTATION PAGE

Form Approved
OMB No. 0704-0188

1. AGENCY USE ONLY *(Leave blank)*	2. REPORT DATE	3. REPORT TYPE AND DATES COVERED
	February 1997	Final report

4. TITLE AND SUBTITLE
Explosion Effects Modeling of Self-Sealing Underground Explosive Storage Chamber Designs

5. FUNDING NUMBERS
DACA39-93-C-0010

6. AUTHOR(S)
Ali Amini, Eugene L. Foster, Colin J. Shellum

7. PERFORMING ORGANIZATION NAME(S) AND ADDRESS(ES)
UTD Incorporated
8560 Cinderbed Road, Suite 1300
Newington, VA 22122

8. PERFORMING ORGANIZATION REPORT NUMBER
UAST-CR-93-005

9. SPONSORING/MONITORING AGENCY NAME(S) AND ADDRESS(ES)
U.S. Army Engineer Waterways Experiment Station
3909 Halls Ferry Road
Vicksburg, MS 39180-6199

10. SPONSORING/MONITORING AGENCY REPORT NUMBER
Contract Report SL-97-1

11. SUPPLEMENTARY NOTES
Available from National Technical Information Service, 5285 Port Royal Road, Springfield, VA 22161.

12a. DISTRIBUTION/AVAILABILITY STATEMENT
Approved for public release; distribution is unlimited.

12b. DISTRIBUTION CODE

13. ABSTRACT *(Maximum 200 words)*

This study investigates the potential performance of self-sealing chambers in rock as a means of containing the blast effects from an accidental explosion in an underground ammunition storage complex. The work was performed as part of the Joint U.S./ROK R&D Program for New Underground Ammunition Storage Technologies. A coherent method for modeling of self-sealing systems is presented. This method illustrated that observations made during field investigations can be incorporated into simulation models for realistic prediction of the behavior of storage chambers during an accidental explosion. The modeling approach incorporated a thermodynamic/numeric technique using a distinct element numerical code (UDEC).

Three self-sealing scenarios were modeled: a sliding block, a weak wall-exhaust drift, and a single weak wall. The performance of the weak wall-exhaust concept was superior to the other designs evaluated. The analysis indicated that this self-sealing design was most successful for reduction of the escaping gas pressure.

14. SUBJECT TERMS

Airblast	Explosive safety
Ammunition storage	Explosive storage
Explosions	Underground chambers

15. NUMBER OF PAGES
60

16. PRICE CODE

17. SECURITY CLASSIFICATION OF REPORT	18. SECURITY CLASSIFICATION OF THIS PAGE	19. SECURITY CLASSIFICATION OF ABSTRACT	20. LIMITATION OF ABSTRACT
UNCLASSIFIED	UNCLASSIFIED		